Networked Power Flower Bell

Energy Harvesting System for a Cybernetic Sound Installation

Diploma Thesis

Institut für Elektrische Anlagen
TU Graz

presented by
Josef Schauer

Advisor
Univ.-Prof. Dipl.-Ing. Dr.techn. Lothar Fickert

Co-Advisor
Ao.Univ.-Prof. Dipl.-Ing. Winfried Ritsch

Director of the Institute: Univ.-Prof. DI Dr.techn. Lothar Fickert

A-8010 Graz, Inffeldgasse 18-I
Telefon: (+43 316) 873-7551
Telefax: (+43 316) 873-7553
http://www.ifea.tugraz.at
http://www.tugraz.at

Graz / March - 2013

Danksagung

An dieser Stelle bedanke ich mich vor allem bei meinen Eltern, die mir meine Ausbildung ermöglicht haben. Weiters gebührt meinen beiden Betreuern, Herrn Univ.-Prof. Dipl.-Ing. Dr.techn. Lothar Fickert und Herrn Ao.Univ.-Prof. Dipl.-Ing Winfried Ritsch, großer Dank für die Bereitschaft, ein nicht ganz konventionelles Projekt zu unterstützen. Sie ermöglichten mir im Rahmen meiner Abschlussarbeit auch einen viermonatigen Auslandsaufenthalt an der *Universidad de Las Palmas de Gran Canaria*. In diesem Zeitraum entstand ein großer Teil der vorliegenden Arbeit. Betreut wurde ich dort von Javier del Pino Suárez, wofür ich ihm sehr dankbar bin. Abschließend danke ich meinem Kollegen und Mitbewohner auf Gran Canaria, Werndelin Klimann. Der stete Dialog über unsere Projekte stellte eine bedeutende Unterstützung dar, die ich nicht missen möchte.

EIDESSTATTLICHE ERKLÄRUNG

Ich erkläre an Eides statt, dass ich die vorliegende Arbeit selbstständig verfasst, andere als die angegebenen Quellen/Hilfsmittel nicht benutzt, und die den benutzten Quellen wörtlich und inhaltlich entnommenen Stellen als solche kenntlich gemacht habe.

Graz, am 20.02.2013

Josef Schauer

Kurzfassung

Energy Harvesting ist die Umwandlung von Umgebungsenergie, die in der Umwelt vorhanden ist, in elektrische Energie [1]. Diese Arbeit beschreibt die kunst-motivierte Entwicklung eines Energy Harvesting Systems für den Einsatz in Klanginstallationen [2]. Als konkrete Motivation dient dabei die Vision des Künstlers Winfried Ritsch: eine Art kybernetisches Blumenbeet, das durch Energy Harvesting versorgt wird. Dem Künstler schwebt die Nutzung einer *Erdbatterie* als Energiequelle vor.

Es ist Teil des Projekts, die praktische Nutzbarkeit dieser Quelle zu untersuchen und gegebenenfalls alternative Generatoren auszusuchen.
Die verwendeten Generatoren liefern, auch abhängig von den aktuellen Umweltbedingungen, sehr kleine Mengen an elektrischer Energie bei – auch zeitlich – stark schwankenden beziehungsweise unterschiedlichen elektrischen Parametern, was es zur Herausforderung macht, diese Energie durch geschickte und sparsame Schaltungstechnik nutzbar aufzubereiten. Es soll auch ein Weg gefunden werden, wie die Blumen miteinander über Funk auf kurze Distanz mit wenig Energieaufwand kommunizieren können, um sich zu vernetzen und gemeinsam musizieren zu können. Dafür werden aktuelle, infrage kommende Technologien verglichen, um schließlich eine passende Lösung zu finden und einzusetzen. Nachfolgend wird das bisher beschriebene System als Power Flower Bell (PFB) bezeichnet. Dieser Ausdruck wird der Qualität, Energie zu sammeln, gerecht, aber die Fähigkeiten des Systems gehen weit darüber hinaus, da man es mit diversen Modulen erweitern kann. So lässt es sich mit verschiedenen Ein- und Ausgangsgeräten verbinden, zum Beispiel Sensoren, um Größen wie Temperatur, Licht, Feuchtigkeit, Schall oder die gewonnene Energie zu messen. In analoger Weise lässt sich eine Vielzahl an Aktoren und Energiespeichern zum Einsatz bringen.

Als Forschungsobjekt soll ein einfaches Modul entstehen, das in der Lage ist, von Zeit zu Zeit (wenn der Energiespeicher ausreichend geladen ist) eine Glocke anzuschlagen. In der künstlerischen Vision ist diese Glocke gleichsam die Blüte der Blume oder ein Teil davon. Dies stellt eine sehr energieeffiziente Art und Weise der Klangerzeugung dar, da das Produkt aus Leistung und Zeit, also die dissipierte Energie, wegen des Impulscharakters des Glockenanschlags relativ klein ist. Es werden die Grundlagen erarbeitet, um ein kleines Netzwerk dieser Systeme realisieren zu können. Es ist naheliegend, alles so klein und sparsam wie möglich zu gestalten.

Abstract

Energy harvesting is the conversion of ambient energy present in the environment into electrical energy [1]. This work describes the art-driven development [2] of an energy harvesting system in sound installations. A motivation for this project is a vision of the artist Winfried Ritsch: A kind of cybernetic flower bed driven by energy harvesting. He is thinking of using an earth-battery as an energy source. It is part of the presented project to investigate the practical usability of this source.
Usually used generators deliver energy according to a wide range of electrical parameters and time, which requires a convenient design to efficiently harvest the small amounts of energy and also leads to the need to use this energy in a smart way (low energy design). To communicate with systems in the proximity, a way has to be found to do so without wires but in a very economic way. Therefore, current low energy digital radio systems are compared. Finally, a technology which fulfils the requirements is deployed. In the following, this item is called Power Flower Bell (PFB), which is able to harvest energy although its abilities go further using additional modules for other purposes. There is the possibility to connect several kinds of input/output devices, sensors to measure temperature, moisture, light, sound, harvested energy as well as plenty kinds of actors and accumulators which store the energy.

As a research object, an extension which is capable to ring a bell (if there is enough energy hartvested) is designed. In the artistic vision, the bell can be seen as the bloom of the flower or a part of it. A bell, due to the impuls-characteristics of triggering, represents a very energy efficient method of sound-generation. The basics for realizing a small network of this plants are described.

Contents

List of Abbreviations

List of Abbreviations

AC	Alternating Current
C	Capacitance
CMOS	Complementary Metal Oxide Semiconductor
CPU	Central Processing Unit
DC	Direct Current
EDA	Electrical Design Automation
FIFO	First-In First-Out
FSL	Free Space Loss
FSK	Frequency Shift Keying
FSR	File Select Register [4]
GPR	General Purpose Random Access Memory
ID	Identifier
ISM	Industrial, Scientific and Medical
L	Inductance
LF	Low Frequency
LR-WPAN	Low Rate Wireless Personal Area Network
MCU	Micro-Controller Unit
MOSFET	Metal-Oxide-Semiconductor Field-Effect Transistor
MPP	Maximum Power Point
MPPT	Maximum Power Point Tracking
OSI	Open Systems Interconnection
PC	Program Counter
PCB	Printed Circuit Board
PFB	Power Flower Bell
PMOS	P-Channel Metal-Oxide Semiconductor

QFN	Quad-Flat-No Lead [5]
R	Resistor
RF	Radio Frequency
RSSI	Received Signal Strength Indicator
RTCC	Real Time Clock and Calender
SFR	Special Functions Register
SPI	Serial Peripheral Interface
TEG	Thermoelectric Generator
Tx	Transmit
UI	User Interface
UWB	Ultra Wide Band
W-LAN	Wireless Local Area Network

1. Introduction

1.1. Motivation

The topic was given by an artistic idea by Winfried Ritsch. His vision is a cybernetic flower meadow, made up by a field of robotic flowers as a kind of cybernetic organism. Each instance of these systems should be powered by the near environment. This should take place in a similar way which real flowers get their energy, like by sunlight or from chemical reactions in the soil. Because this obviously is a low-power source, *Energy Harvesting* is the ultimate key word. In detail, Ritsch is thinking of mainly using the *dirt-battery* described in section 3.1. Through RF communications, the plants should be able to realize a musical composition together which (also) depends on their state. The artistic idea is described in a separate document by Winfried Ritsch [6].

1.2. Problem Statement

The energy sources which drive the PFB should be chosen to come as close as possible to a natural plant in its behaviour and look. The *dirt-battery*, described in section 3.1, is able to fulfil this need because the electrodes can be seen as *roots* of a plant. *Dirt-battery* and *earth-battery* mean the same in this work.
Dug in the soil and watered from time to time, they are the source of energy for the plant. Unlike the concept of the soil lamp [7], the intention is to avoid a serial cell-structure since all of the plants should be planted in a soil outdoors, otherwise it would be very hard to divide the soil in cells. Instead of switching several cells in series, the challenge is to investigate the effects of increasing the surface of the electrodes taking part of the process. This – electrically – is equivalent to switch several cells in parallel. The next issue is to bring the low-output voltage (in a zinc-copper environment about 1,1 V) to a level which can run low-power devices. The dirt-battery represents one kind of energy source. Any Direct Current (DC) sources can run the presented circuit which runs the harvested energy in a smart way. This project should be the proof that the concept of harvesting energy and consuming it in a low-power way for RF communications and sound generation by bells is possible.

1.3. State Of The Art

Harvesting usually means collecting ripe fruits. The harvesting of energy is for example already taking place in bicycle dynamos and piezoelectric gas lighters. In both cases, energy that is present anyway is used to obtain a certain amount of electricity. Of course, the generation of electricity appears as an additional mechanical resistance to the user or the system that converts energy. Energy harvesting is the use of ambient energy to create electricity for a small or mobile equipment. Solar cell *photo voltaics* on space vehicles can also be seen as energy harvesting devices [8]. In the classical sense, energy harvesting is supposed to label sources like piezoelectric generators which convert mechanical to electrical energy like in modern switches.
A loudspeaker which converts changes of the air pressure to mechanical movements of the membrane can be used to convert acoustic energy to electrical energy by a coil and a magnet mechanically connected to the membrane [9]. The generation of electrical energy by *Seebeck* elements (they generate a voltage through a temperature gradient using the *Seebeck* effect) and photo voltaics is already quite common, for example in sensor nodes. The dirt-battery was already used, for example for a lamp [7] or a clock [10]. There are several cells in a serial connection, which permits a higher output voltage at a certain current or a higher current at a certain voltage. The cells are made up of conventional copper and zinc electrodes in a soil, and sometimes they have to be watered.
In this work, it is intended to find a way to obtain enough energy for the mentioned tasks by using just one galvanic cell and convert the low output voltage to useful levels. You can see the *Soil Clock* in figure 1.1.

Figure 1.1.: The soil clock by Mstaps [10]

1.4. Research question

It shall be shown that it is possible to build up a networking sound installation powered by energy harvesting concepts with a low power DC source. This work should deliver a guide line for similar projects in the future. Applications for energy harvesting systems are almost never-ending, having in mind that there is NO restriction in using any available energy source at almost any available output power. It is also quite important to mention that the thinking of energy-harvesting should not be restricted just to electrical systems, much more motivation should be given to use energy more often in the form in which it appears as directly as possible – for example it must be more efficient to use thermal energy directly for heating, than converting it to electricity for running electric heating systems. Also mechanical power which often appears in our nature and everyday-life could be used or even stored in a more efficient way than by converting it to electric energy before storing.

1.5. Scientific Interests

Because of the modular flexibility, the access to solutions for realizing energy harvesting sound installations or sensor/actor nodes increases by analysing the technology. The great advantage of energy harvesting systems which is noticed by the industry is the fact that there are no costs for changing batteries any longer. The knowledge of how to apply energy available in the direct environment of a system to build up a sound installation which is networked via RF can help to develop a wide spread of useful systems which do not just serve as sensors like as already applied in a lot of cases in industry, but also as actors which of course can just act when there is enough energy available. For a swarm or a cluster of items, this also requires research on how they can communicate. Another motivating fact is that by running a copper-zinc galvanic element in a copper-polluted soil – as you can find it for example on many traditional wine yards – the zinc will be left in the soil and the copper will be united with the copper-electrode, so the Power Flower Bell represents a nice-sounding detoxification method for contaminated soils.

1.6. Methods

By measuring the output at several circumstances, the earth-battery is investigated empirically. This makes sense since the goal application will take place on a meadow [6], which means that you will not find a laborious defined environment but a natural one. These facts imply that care has to be taken so that other species can still live on and in the soil in the future. Furthermore, a chip is found and implemented to convert the output source of the dirt-battery to a useful value. The heart of the system, a microcontroller and peripherals, is realized on a PCB and programmed. All the software

environment used for writing this paper as the programming of the micro-controller is open-source software based on ubuntu Linux. For the first PCB version described in chapter 7 the Software *PADS* by *Mentor Graphics*®, was used.

1.7. Structure of the Diploma Thesis

In chapter 2, the block diagram of a PFB is presented. Low power RF systems are discussed. The next chapter, chapter 3, gives an overview of the most common sources for energy harvesting systems. How the obtained power is prepared to run an electronic system is illustrated in chapter 4. In the following, the main electronic components, a *PIC*®*16LF1823* micro-controller from *Microchip*® and a *MRF89XAM8A* RF module, are explained. Finally, the realization of the PFB as an electronic circuit is summarized.

2. System Overview

2.1. System Block Diagram

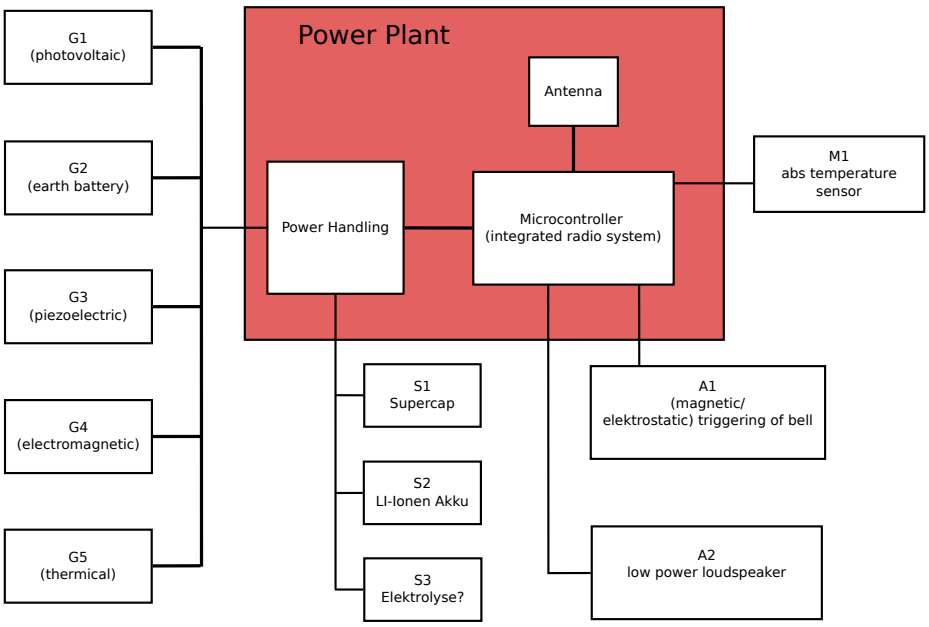

Figure 2.1.: Block diagram to summarize the Power Flower Bell (PFB)

Figure 2.1 presents a universal block diagram of the power plant in an early evaluation step. It shows possibilities to use the PFB. PFB in this work means a PCB, which was developed and is equipped with the described components. The source(s) and an actor have to be connected on prepared headers. This work is concentrated on the use of a dirt-battery (3.1) as an energy source. The actually developed circuit is able to be powered with any DC source up to 3 V. For using an Alternating Current (AC) source, like a piezoelectric or an electromagnetic one, the power handling block has to be modified.

The application of AC sources is not a topic of this work.
One can find a summary of common energy harvesting sources in chapter 3. The micro-controller that was finally chosen has no integrated RF-system but instead an all-in-one low-power RF-module, which is controlled by the micro-controller via Serial Peripheral Interface (SPI), is applied. This decision was made because a modular system was desired. The temperature sensor, the loudspeaker and the microphone are not implemented in the PFB. An actuator can be controlled by a mounted Metal-Oxide-Semiconductor Field-Effect Transistor (MOSFET) in order to trigger the bell.
Energy storage is a topic with an enormously increasing need. In energy harvesting systems, mainly supercaps and Li-Ionen accumulators are used to store electrical energy. This topic is treated in chapter 4.

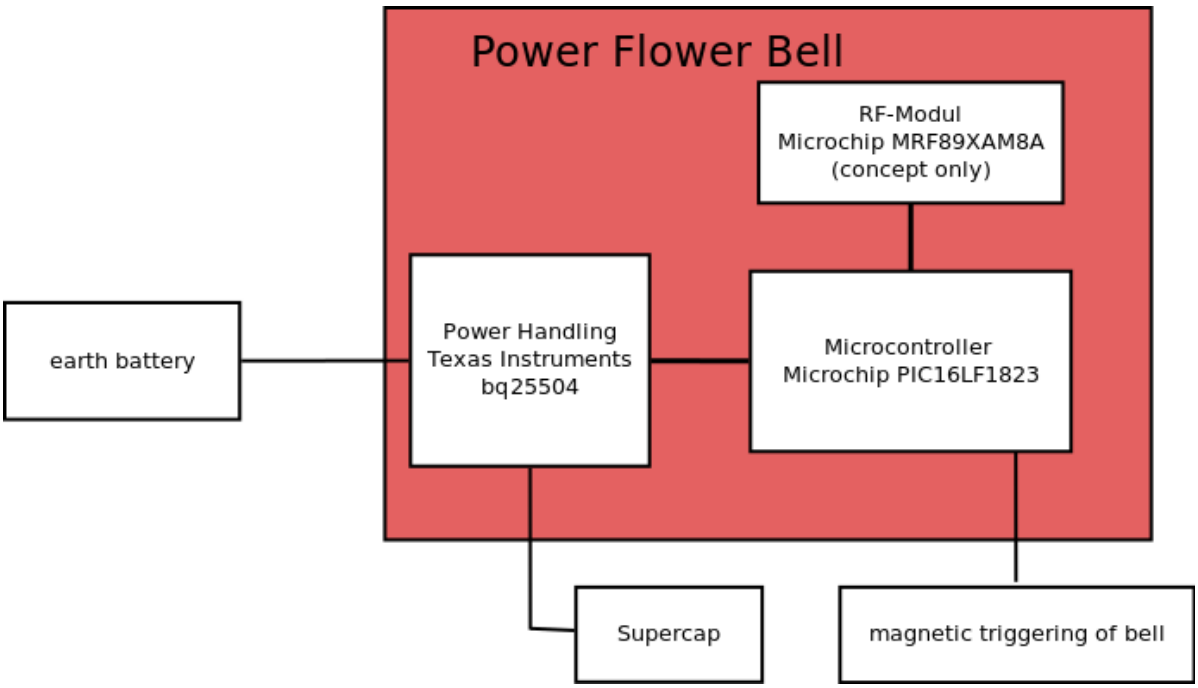

Figure 2.2.: Block diagram of the finally implemented PFB

2.2. Power-Handling

The power-handling block converts the low output voltage of the source to a higher level. This voltage is loaded to a battery or supercap. The challenge in using low-power output energy sources with energy harvesting modules like the *bq25504* from *Texas Instruments Incorporated* is, that they have to deliver enough voltage and power to keep the module running in capturing and storing. In the case of the dirt-battery, this means, that there is a minimum configuration (dependent on the surface of the zinc and copper electrodes as the concentration of copper sulphate in the earth and humidity)[11]. Below this

configuration (measurable in the *no-load* or *open loop* voltage of the source) the *bq25504* will not be able to load the storage element to a higher voltage than a certain value in its range. At this point, there is just enough energy to compensate the losses (this effect was absolutely notable in the experiments with dirt-batteries).

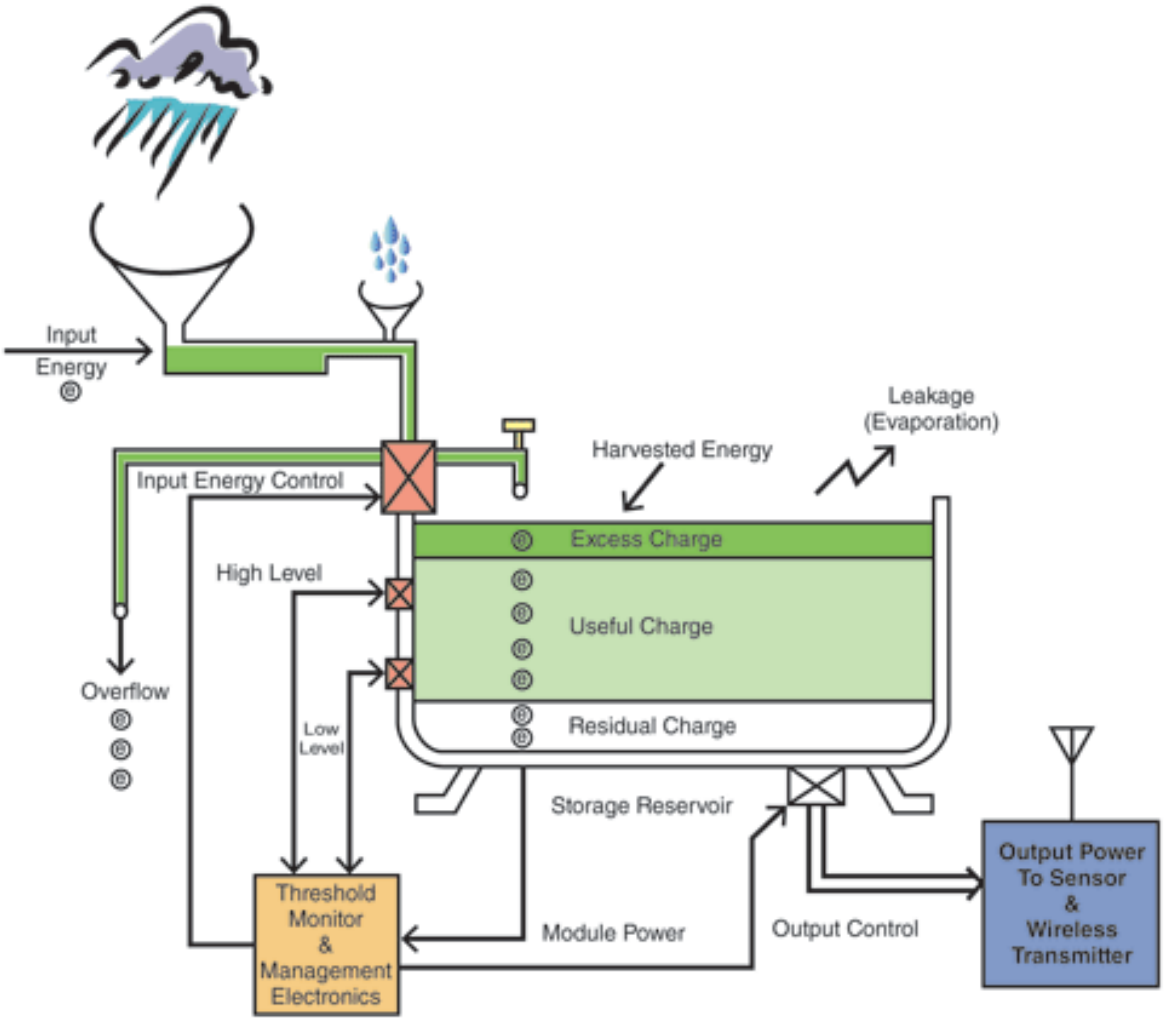

Figure 2.3.: Concept of energy harvesting [11]

Figure 2.3 shows what happens with the energy in an energy harvesting system. The circumstances correspond quite exactly with the task of the *bq25504* in the PFB. Note the leakage, drawn like evaporation: it is always present but, intended to keep as low as possible by using small capacitors with low leakage, small series resistors and high value resistors for set-up. The overflow, in case of the *bq25504*, is very low because it just uses current of the source to maintain an upper voltage limit, which is programmable. There is no actual overflow but a compensation of losses.

2.3. Ultra Low Power Radio Frequency

As described in the artistic idea [6], a wireless network should be formed by a crowd of copies of the developed system. Since the idea is to act very economically in the sense of current consumption, especially RF applications have to be done in a very smart way. Therefore, the nowadays very common ultra low power RF technology should be used. This technology differs in the way that the current consumption is much less than with common RF transceivers. Energy saving is achieved mainly by very few on-time of the transceiver as by the high efficiency of newer silicon-RF chips [12]. To use very little power, systems should just communicate with neighbours or closer devices. By passing the information from each one to the next, the idea of the *Map Of the Known World*, treated in subsection 2.3.6, can be realized.
Industrial, Scientific and Medical (ISM)-bands are frequency bands that can be used freely, but there can be data losses because other devices which also use the same frequencies can disturb communication [13]. ISM frequencies are for example 27 MHz, 433 MHz, 868 MHz and 2,4 GHz, just to mention the most important ones.

Because of earlier experience with such devices, there was ambition to use a microcontroller from the *PIC*® family of *Microchip*® to control the PFB. The search of their product range for low power RF solutions brought two interesting possibilities, the MRF24J40MA, which is a 2.4 GHz IEEE Standard 802.15.4™ RF-transceiver module and the MRF89XAM8A, which is a 868 MHz Ultra-Low Power Sub-GHz Transceiver module. Both of them offer an integrated peripheral circuit and an antenna, so they can be used out of the box. Control is achieved by SPI communication. Finally, the *MRF89XAM8A* (3.3 V typical) was chosen because it consumes much less current in RX mode (3 mA), compared to the 19 mA of the MRF24J40MA (3.3 V typical in both cases). The same accounts tor the sleep mode in which it consumes 1 µA, half of the current driven by the MRF24J40MA in the same mode. From the economic point of view, the actual prices for both devices are around € 7, depending on the reseller and amount of orders. The choice permits a quick and easy set-up since there is a lot of useful documentation available for *Microchip*® hardware. There is no need to design the RF part because it is completely integrated into the module. When it is about to develop an open-licensed RF solution, it is common to use the ISM bands. For these frequency bands, there are just rules for the power they transmit as for interfering with neighbours frequencies. In Europe, in the Ultra High Frequency (UHF) band, you can choose the bands between 433,05 MHz and 434,79 MHz, between 863 MHz and 870 MHz; in the microwave area, the 2.4 GHz is the most common for techniques like Zigbee™, Bluetooth™, Wireless Local Area Network (W-LAN) etc. [14]. The subGHz frequency band is chosen because it delivers 8.5dB less free space loss than the 2.4 GHz frequency. Furthermore, the 2,4 GHz wavelength means higher diffraction losses [3] than the sub-GHz solution.

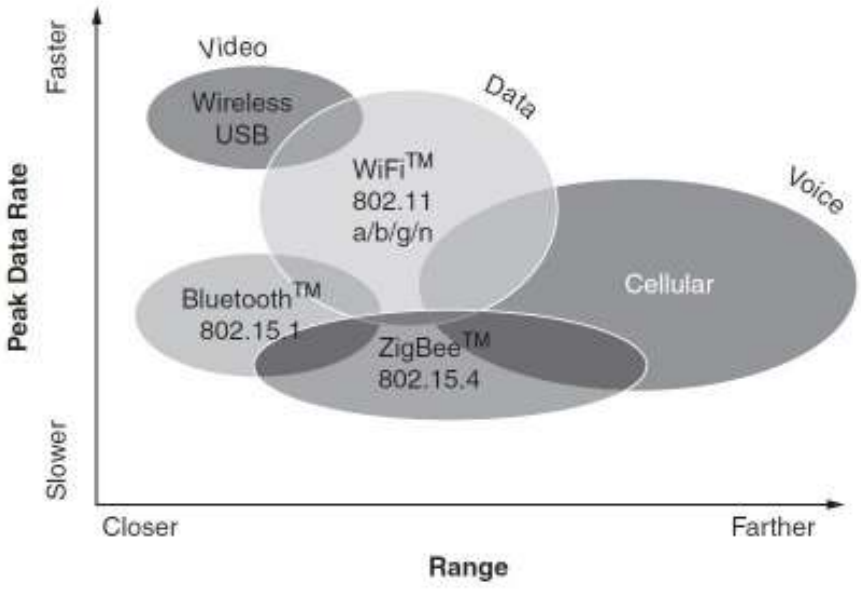

Figure 2.4.: A raw order of common wireless network types [15]

2.3.1. RF wave propagation

It is important to have knowledge of how the transmitted wave circulates in space to realize a *Map Of The Known World* with low power consumption. By estimating the distance to a transmitter, knowledge of the constellation of other PFBs can be gained. Actually, of course the best case is to have the widest range with the least power. But the range should be well-known.

2.3.1.1. Large-Scale Fading

This part of the document helps to calculate the average signal strength from the transmitter at a given distance. The **free space** loss in a clear Line-Of-Sight (LOS) can be calculated easily.

$$EIRP = P_t \cdot G_t \tag{2.1}$$

$EIRP$	Equivalent isotropically radiated power [3]
P_t	transmitted power; 10 dB (typical)
G_t	antenna gain transmitter; -0,855 dB typically for *the MRF89XAM8A* [16]

The output power of the *MRF89XA* Integrated Circuit (IC), which controls the *MRF89XAM8A* module, is not sensitive to the supply voltage but it depends on the temperature. There is more output power when the temperature is higher. In the range between 0 °C and

85 °C, the output power varies in a range of about 2,5 dB [16]. The transmitting power is estimated based on the data in the data sheet of the *MRF89XA* [17]. It says that the Power Amplifier (PA) block is supplied by a regulated 1,8 V-supply. Connected to a 50 Ω antenna, the current is supposed to be

$$I_\mathrm{t} = \frac{U_\mathrm{t}}{R_\mathrm{ant}} = \frac{1{,}8\,\mathrm{V}}{50\,\Omega} = 36\,\mathrm{mA} \tag{2.2}$$

The transmission power is

$$P_t = U_\mathrm{t} \cdot I_\mathrm{t} = 1{,}8\,\mathrm{V} \cdot 36\,\mathrm{mA} = 64{,}8\,\mathrm{mW} \tag{2.3}$$

The antenna gain G_t is given by the datasheet of the MRF89XAM8A module in dB

$$\text{-}0{,}855\,\mathrm{dB} = 20 \cdot log(G_t) \Rightarrow G_t = 0,906 \tag{2.4}$$

Finally, the equivalent isotropically radiated power ($EIRP$) is obtained.

$$EIRP = 64{,}8\,\mathrm{mW} \cdot 0,906 = 58{,}71\,\mathrm{mW} \tag{2.5}$$

With these data, it is possible to calculate the Power flux density in $\mathrm{mW/m^2}$. Note: This is for calculating an isotropic antenna, which is not the case for the antenna of the *MRF89XAM8A* because it is a PCB on-board antenna as you can see in the following picture. It is taken from the data sheet of the *MRF89XAM8A* [16]. *Microchip* used an *Ansoft Designer* and *HFSSTM 3D full-wave solver software* by *ANSYS Inc.* (www.ansoft.com) to design and simulate the PCB antenna.
Figure 2.6 shows the simulated 3D pattern of this antenna. It compares the power radiated in every direction relatively to the power that would be radiated by an isotropic antenna at the same power. An isotropic antenna is an antenna that radiates its power uniformly in all directions [18].

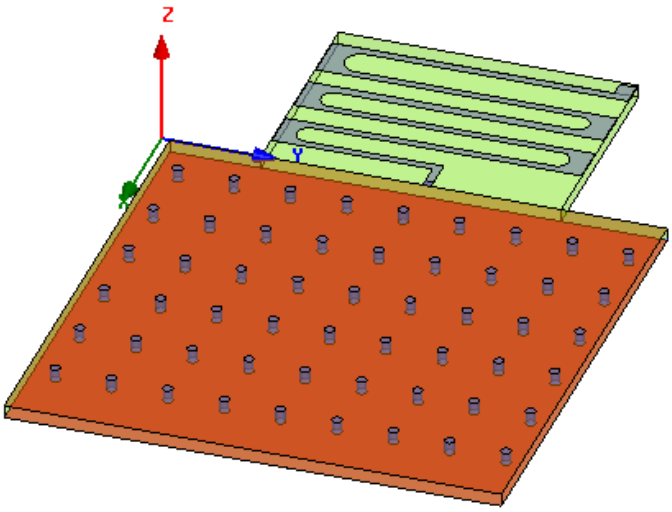

Figure 2.5.: The used model for simulating the *MRF89XAM8A* PCB antenna [16]

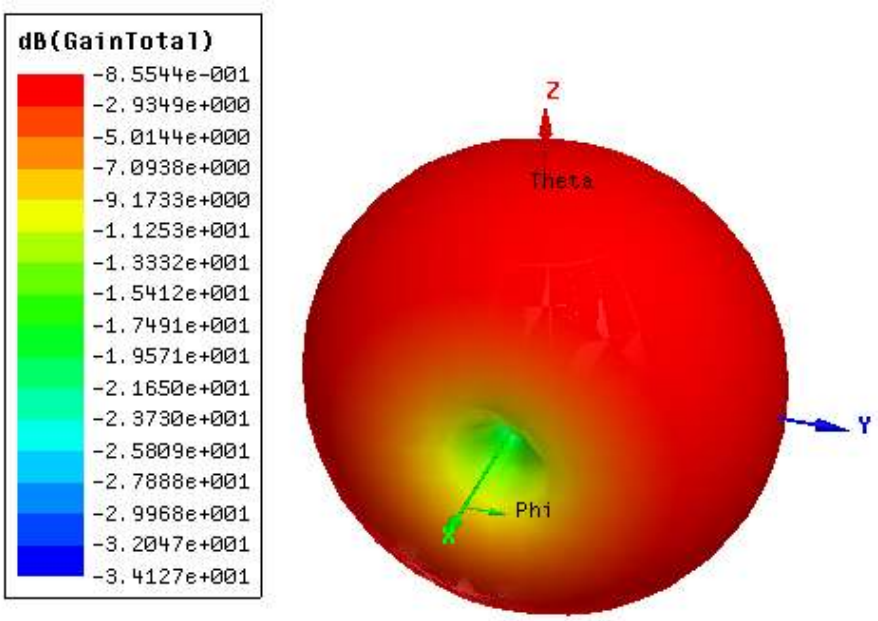

Figure 2.6.: 3D radiation pattern simulated [16]

$$P_d(d) = \frac{EIRP}{4\pi d^2} \tag{2.6}$$

P_d	Power flux density	mW/m^2
d	distance between transmitter and receiver	

With the data calculated before, this gives

$$P_d(d) = \frac{58{,}71\,\mathrm{mW}}{4\pi d^2} \tag{2.7}$$

The received power is calculated for an isotropic antenna with the antenna gain taken from figure 2.6 in the yz-plane. This approach is possible because the antennas of the PFB will be mounted with the x-axis in figure 2.5 and figure 2.6 in vertical direction.

$$P_r = P_{\mathrm{d}}(d) \cdot \frac{\lambda^2}{4\pi} \tag{2.8}$$

P_{r}	received power
λ	wavelength [m]

with

$$\lambda = \left(\frac{c}{f}\right) = 0{,}3453\,\mathrm{m} = 34{,}53\,\mathrm{cm} \tag{2.9}$$

c	speed of propagation (299 792 458 m/s)
f	Frequency (868 MHz)

The free-space loss Free Space Loss (FSL) can be calculated.

$$FSL = \frac{EIRP}{P_r} = \left(\frac{4\pi \cdot d}{\lambda}\right)^2 = 1324,42 \cdot d^2 \tag{2.10}$$

$$FSL[\,\mathrm{dB}] = 10 \cdot log\left(\left(\frac{4\pi \cdot d}{\lambda}\right)^2\right) = 20 \cdot log\,(36,39 \cdot d) \tag{2.11}$$

Equation (2.8) and equation (2.7) were used to get this simple expression. It is used for the *Map of the Known World* in subsection 2.3.6.
Hint: For the calculations above, lecture notes of the course *Wireless communication networks and protocols* are used [3]. This course is lectured by Dipl.-Ing. Dr. Johannes Ebert for the *Institut für Kommunikationsnetze und Satellitenkommunikation* at the *Technische Universität Graz*. During researches, it was necessary to contact him to correct [3], as the fraction in (2.10) was presented in the wrong way.
In the following, several common low power RF technologies are presented. This should serve as a pool of ideas for implementing the network in our system.

2.3.2. Communication Protocol Layers [3]

Very wide-spread is the ISO 7 layer Open Systems Interconnection (OSI) model. Two of these layers are specific for wireless networks.

- **Physical Layer:** It defines the transmission of raw bits, the frequencies used as the bandwidth and modulation, the spectral shape of the signal Forward Error Correction (FEC) coding. This layer also determines frames and bursts and adds symbols which are used for synchronization. Furthermore, it provides the decided bits to the upper layer, which means that there might be bit errors.
- **Data Link Layer:** This layer defines the packets for transmission, for example Internet Protocol (IP) packets. The addressing and switching for this layer is organized, and it passes information to the receiver. For the transport units in the physical layer, the data link layer fragments and reassembles the packets. The integrity of data is ensured (for example by a Cyclic Redundancy Check (CRC). If there was an error in transmission, this layer cares about transmission repeats (Automatic Repeat Request (ARQ)). Access of Media Access Control (MAC) is task of this layer. Of course, this layer hands received packets to the network layer, which implicates that packets can get lost but usually do not have bit errors.

A very important strategy in this context is the one of Carrier Sense Multiple Access/-Collision Detection (CSMA/CD): Every device can have access to the others. In case of collusion one has to wait for a random time period, then start a new try. In the case of the PFB, the time is not a random value but a characteristic value for every single device. It can be compared to the case of a telephone call: If both partners start talking at the same time, they stop talking and wait for an undefined time duration. Then, one of them starts talking again.

2.3.3. ZigBee®

ZigBee® is a kind of technology that comes from the IEEE 802.15.4 standard. This standard is defined for low-bit rate and extreme low power [19]. It is mainly supposed to work in industry and home and building automation. It is similar to the 802.11 standard for W-LANs and *Bluetooth*™ but especially shaped for the mentioned applications. The transmission rate is less than 802.11 or *Bluetooth*™, but also the current consumption is less because many applications work with batteries, which is a critical topic. The protocol stack of *ZigBee*® is less complex than the one of *Bluetooth*™, although there are still some known to be less complex, like the *MiWi*™ Protocol by *Microchip*. From sleep-mode *ZigBee*® wakes up faster than *Bluetooth*™.
Ultra Wide Band (UWB), defined by the Federal Communications Commission (FCC), is a signal with a bandwidth of more than 500 MHz in the frequency range of 3.1 GHz to 10.6 GHz, a RF method with a bandwidth of more than 25% of the carrier frequency or a carrier frequency of more than 1.5 GHz.
What is special for *ZigBee*® is that in the UWB, it is possible to transmit coded

signals over a wide spectrum. This is called Low Rate Wireless Personal Area Network (LR-WPAN), developed for industrial production, vehicles and commercial technologies and delivering self-configuring sensor and actor nets, redundancy and increased transmission range by Multi-Hopping. LR-WPAN is based on standards defined by the IEEE 802.15.4. Because the carrier is suppressed, power can be saved (up to two thirds) compared to methods without suppressing the carrier frequency [20]. Also, because inactive components are turned off in *ZigBee*®, current consumption in the active mode of 15 mA is possible.
There are two types of communication:

- **Beacon-mode:** nodes are requested continuously at certain points of time
- **Non-beacon-mode:** nodes are active just at certain actions, like a sensor input etc.

With *ZigBee*®, maximum distances between 10 m and 75 m are possible. *ZigBee*® delivers multiple steps for security, which is an important topic in industrial use.

2.3.4. ANT™ Protocol

ANT™ works in the 2.4 GHz ISM band and is designed for low power applications powered by batteries maintaining the robustness of a real wireless protocol. This includes:

- sophisticated co-existence mechanisms
- practical topologies going further than star and peer-to-peer
- proximity-based pairing methods
- seamless transfer of bulk data from one device to another [21]

ANT™ is a fundamental building block of *ANT+*™ [21].

A typical *ANT*™ node exists in an *ANT*™ chip and a Micro-Controller Unit (MCU) with peripherals like an antenna and a power supply. A logical connection between two *ANT*™ nodes is called *ANT*™ channel. A network can be formed by multiple channels without a coordinator or a master, therefore, the channels are called fully independent. *ANT*™ nodes can act as multiple channel endpoints with master/slave combinations which are dynamically created and destroyed because these channels are ad-hoc[1]. An *ANT*™ channel is built up between a master and a slave endpoint.
The master initiates the communication and controls the channel, often it is called the primary transmitter, since, at a specific channel period (0.5 Hz to 200 Hz, defined by the MCU), it sends a data packet which has exactly 8 byte of application payload.
The slave point accepts the communication and, therefore, it is also called primary receiver. When detected a master transmission, it gets synchronized to the master with

[1] Ad-hoc Network just exist for the time in which a communication takes place. They organize and set them up on their own. [22]

the channel period of the master or a multiple of it. Like this, the slave just transmits data if it is instructed to do so by the MCU.

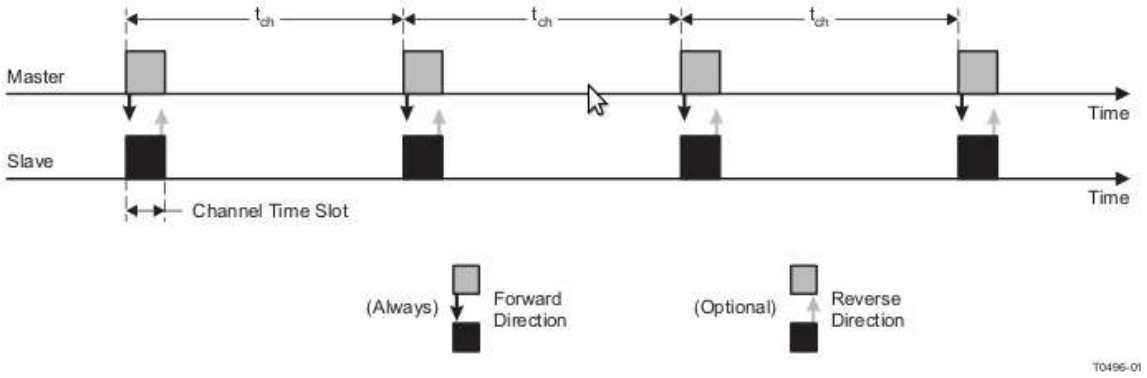

Figure 2.7.: Timing of an ANT^{TM} channel [21]

An ANT^{TM} packet exists in the following parts which are set up by the host MCU:

- 8-byte data payload
- Frequency (2400 MHz)
- 2-byte network key proximity-based pairing methods
- 4-byte channel Identifier (ID)

There are 4 types of channels which fit different applications.

- **bidirectional:** Master and slave can transmit data in the way described in subsection 2.3.4
- **unidirectional:** Just the master transmits data by using broadcast messages
- **shared:** This bidirectional channel permits a single master to address up to 64K slaves, every slave synchronized to the master channel period. Two bytes of the data payload are used to address the slaves, also broadcast is supported. This type of channel is suggested for networks with a lot of nodes and which are critical in meanings of power consumption.
- **scanning:** asynchronous; they do not synchronize to the master, but every message from any master is given to the application.
  - **continuous scanning** means that the receiver is always turned on and is suitable for communications in which one end is not critical to power. Delivers low latency.
  - **background scanning:** Without being synchronized to any channel, continuous transmissions are searched. Much less power consumption compared to the continuous scanning, and data latency is increased. Well-fitting for low power devices which have to communicate with multiple nodes at reasonable latencies.

ANT^{TM} comes up with three types of messages:

- For **broadcast** messages, no response is necessary, so any device which sends a broadcast has no information about whether the message was received well or not. It is the message type with the lowest power consumption. Broadcast messages can be sent to several devices at one time and are useful for applications in which information of slowly changing values has to be sent.
- **Acknowledge** messages expect and provoke a response, which is managed by the ANT^{TM} protocol. That means it is passed to the MCU and provides information if the message was received successfully. If there are messages which are not confirmed, retries are in the hands of the MCU.
- If a bulk of data shall be transmitted very fast, the **burst** message type is a worthy option. Still able to be powered by a coin-cell battery, it begins to transmit data on a channel-period time slot. Since the intention is to send the data as fast as possible, this period can be extended. The burst packet which can send up to 20 kbps will be re-tried by ANT^{TM} five times if necessary, and the MCU is informed whether data was received well or not.

An important feature of ANT^{TM} is the ability for pairing.

This method is a task for all wireless technologies and allows ensuring that a slave talks to the right master. It is necessary that the slave knows the channel ID of the master. In the case it does not know the master channel ID, it can be obtained by pairing. Several types of pairing exist:

- **wildcard:** The channel ID is set to 0. In this mode, the slave will connect to the first master it finds. It is a very simple and transparent method, the user just has to do a User Interface (UI) operation and will then be connected to the master. This method will not serve in areas with more than one master because the device can easily be connected to a master which does not belong to the slave. The possibility of getting connected with a wrong master can be reduced by putting the ANT^{TM} channel in a pairing mode. ANT^{TM} supports the pairing mode by setting a certain bit in the master's channel ID and the slave is just allowed to connect to masters with this bit set. In practice, it is not that useful because the usability is reduced (one UI operation on the master device and another one on the slave is necessary).
- For this work, a very interesting kind of pairing is the one which takes place between a slave and a master, depending on the proximity, hence called **proximity pairing**. ANT^{TM} delivers a simple interface for defining a proximity threshold and permits the blocking of other devices outside the threshold. This type of pairing is very efficient, seamless to the user and permits work without any UI to be installed.

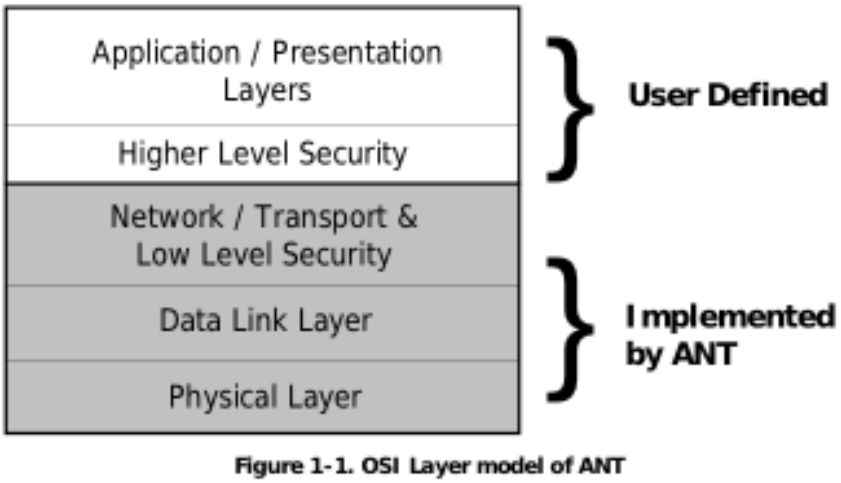

Figure 2.8.: OSI layers of ANT [23]

2.3.5. DECT ULE

Digital Enhanced Cordless Telecommunications Ultra-Low-Energy (DECT ULE), actually a pure telephone standard but now also data transfer and internet via Cordless Advanced Technology - internet and quality (CAT-iq) is realized. This standard works in a protected frequency area, in Europe between 1880 MHz and 1900 MHz [24].

2.3.6. Map of the Known World

The *Map of the Known World* is an idea by Winfried Ritsch and presented in [25]. A network should be used to form a swarm. The network should be self-determining and growing. By the range of the RF and the Received Signal Strength Indicator (RSSI) implemented in the *MRF89XAM8A*, it is possible to estimate the distance to a device. The devices remember the others with which they are communicating. This data can be interchanged with neighbours, and – as there is enough memory – every node can earn knowledge of the position of the others.

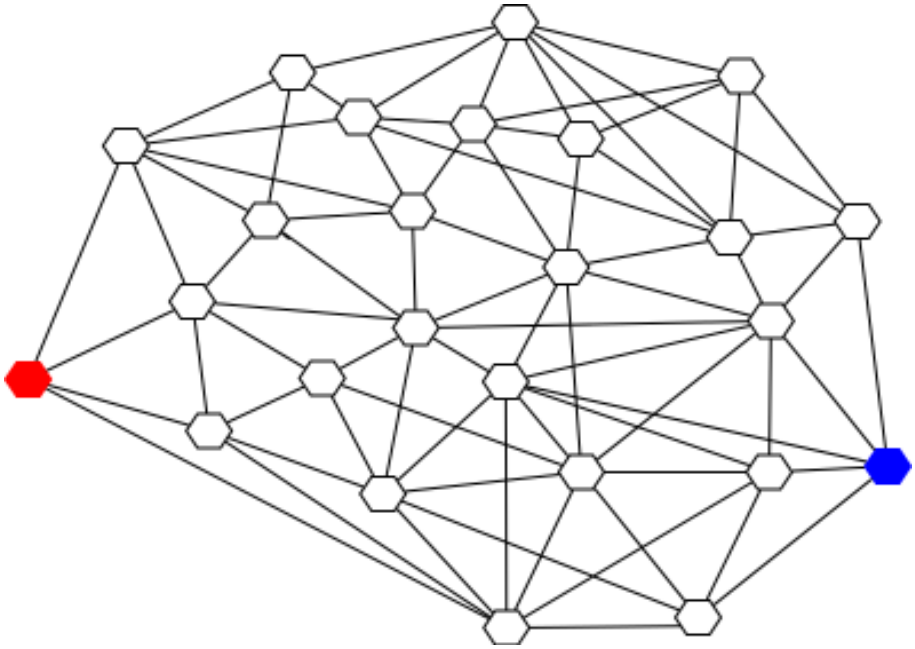

Figure 2.9.: The main idea of the *Map of the Known World*

The communication is realized with ultra-low power RF technology. In order to just use as little energy as possible – this is the concept for anything the PFB does, all the system has to pass as much time as possible in a sleep mode. This especially is valid for the RF task, which needs – relatively to the rest of the system – a lot of power. A long sleep time is achieved by synchronization of the units and being RF active just during certain time slots. The synchronization is achieved by the RTCC (subsection 5.2). Consider a PFB, which starts after a reset: It will harvest energy until VBAT_OV is reached. Before VBAT_OV is reached, VBAT_OK is set high. This signals to the micro-controller that there is enough energy to intend communication. But it has to wait, for synchronization reasons. When a synchronization time slot appears, it sends signals and waits for responses. The PFB starts with a very low power setting. If there is no response, the next time it sends with more power and so on. Like this, and by using the RSSI, an estimation of the distance to the responding PFB is possible. Moreover, data is gained of how much power is needed to send data to a device. All this data is saved in a list and interchanged with the communication partners. A use-case for this scenario is illustrated by Winfried Ritsch in figure 2.10.

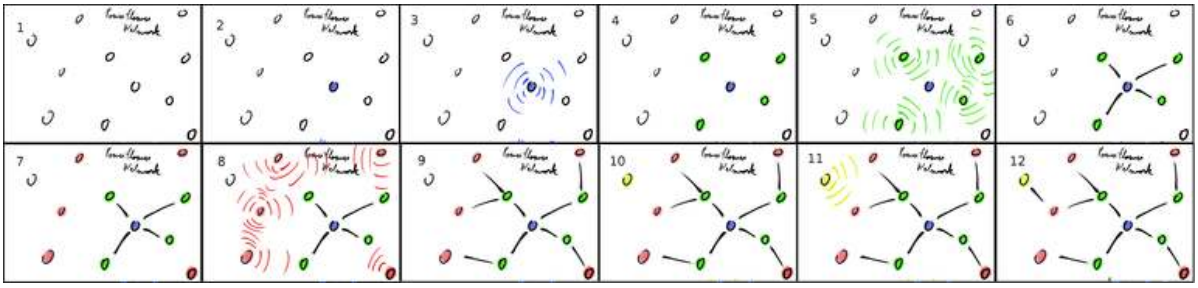

Figure 2.10.: Visualization of an auto-generated network by the PFBs [25]

3. Energy Sources

Usually, energy harvesting today is supposed to mean electronic systems that work by converting energy present in their ambience into electrical energy. This can be done using physical effects like induction, electrostatics, piezoelectricity, photo electricity or the *Seebeck* effect [26].
Also, there is the possibility to obtain electrical energy using chemical or biological sources, a field of science that is increasing [27] [28].
This project is focused on a source called *dirt-battery*, explained in more detail in section 3.1.

For the delivered system, it is possible to replace or tune up the energy source with solar panels or thermoelectric elements working with the *Seebeck* effect just by modifying the set-up of the harvesting chip, which is done by a few resistors. The mentioned harvesting chip is a *Texas Instruments bq25504Ultra Low Power Boost Converter with Battery Management for Energy Harvester Applications*, thought for a wide range of input voltages. All three kinds of generators have similar characteristics (a DC output which depends on the environment around them). This type of source is the one which is supported by the chip. Figure 3.1 helps to get an impression of the order of power per volume of different principles.

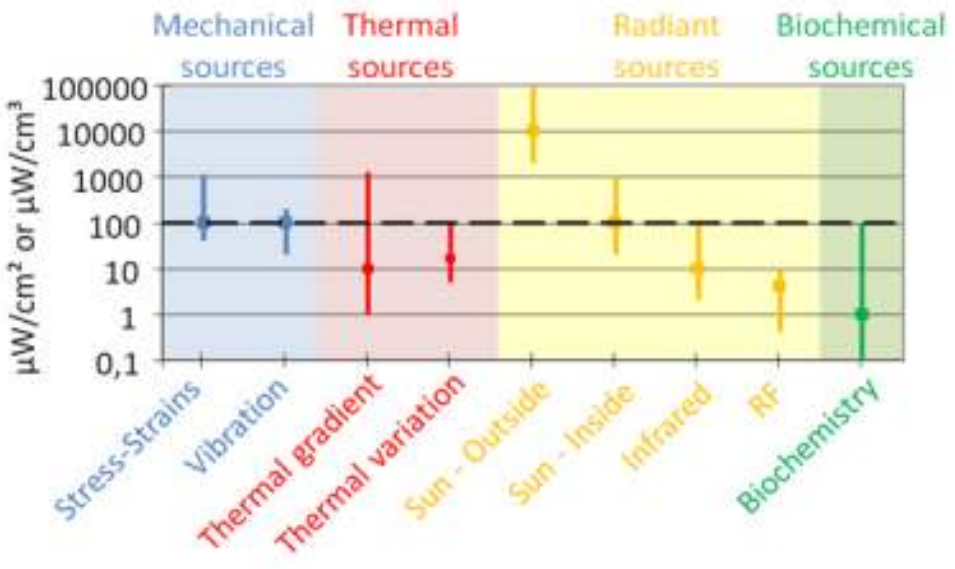

Figure 3.1.: Energy sources compared by their power densities [29]

3.1. Dirt-Battery

The idea of the dirt-battery is based on the galvanic cell (described in subsection 3.1.1). Just by putting two electrodes of different metals into the ground, it should be possible to harvest enough energy to power the PFB. The dirt-battery is not a new idea [30], it was first demonstrated in 1841 by *Alexander Bain* [31]. He powered a clock with a dirt-battery. Actually, there are two ways of using soil to generate electricity. This work just takes a look at the method in which the soil serves as an electrolyte, like it was done in the days of *Bain*.
Nowadays, there are already found microbes that produce electron flow, like *Shewanella oneidensis, Rhodoferax ferrireducens* and *Geobacter sulfurreducens*. They appear naturally in the soil and, by breaking down their food, they produce electrons which they even carry from one place to another [31].
The output power of the earth-battery is not constant, it depends on factors like the connected load, the state of the electrodes, the state of the soil, in which they are *planted* in, as the distance between the electrodes. It is not possible to determine the exact condition of the used soil. It makes sense to investigate the electrical behaviour of this source in a real application to find a way to extract the current in an efficient way. The results of experiments done with different set-ups are summarized in subsection 3.1.3. Furthermore, the electrodes should be placed into the same soil, that the separation of the half reactions can just be achieved by varying the distance between the electrodes.
Similar and well-known are experiments like the lemon battery [32]. It is possible to light a 5 mm standard Light Emitting Diode (LED) by a serial set-up of two lemon batteries. Of course, other fruits can be taken, hence the output will be different, but in principle, the open-circuit voltage mainly depends on the material of the electrodes. The amount of acid and the possibility of interchanging electrons determines how much current can flow and limits the power which can be provided by such a battery.
The fruit-devices give motivation, that also the dirt-battery can be used without additional arrangements to separate the two half-cells.

Another valuable inspiration for the dirt-battery can be found in the *Daniell* cell, which is made of a piece of zinc placed in zinc-sulphate inside a bowl made of clay. This bowl is placed in copper-sulphate inside a copper bowl. The clay pod serves as a diaphragm which permits a transport of ions but does not permit a transport of electrons. So, electrons are forced to be moved externally through a conducting connection between the electrodes. A six-cell Daniell element is shown in figure 3.2.

Figure 3.2.: A Daniell Element with six cells [33]

A pod made of clay can easily be mounted into the soil. That is the reason why this possibility is also investigated empirically.

3.1.1. Redox reaction

Oxidation is a chemical reaction in which a material electrons are abstracted, reduction is a chemical reaction in which a material electrons are added. Redox reaction is the term for a chemical reaction in which electrons from one material are transferred to another one. This results in a change of the oxidation number of the materials involved in the reaction. The transport of electrons is the most important effect in a redox reaction, but besides, there can be a transfer of atoms and ions. The reducer is the electron donor, and the oxidizer is the so-called electron acceptor.

By putting a piece of zinc in a solution with Cu^{2+} ions, a spontaneous redox reaction in which metal copper is sedimented on the piece of zinc, is obtained. The zinc in this process is dispersed.

In figure 3.3, you can see a galvanic cell which works with the same redox reaction of zinc and copper, but there is no direct conductance between the zinc and the Cu^{2+} ions. In one tank, the zinc electrode is in contact with the Zn^{2+} ions, while in the other one, the copper is in contact with the Cu^{2+} ions. That is why the reaction can just take place due to electrons moved from one electrode to the other by connecting them externally. By separating the reduction and oxidation half-reaction, an external electron flow is

generated. The electrode on which the oxidation takes place is called anode and the one on which the reduction is situated is named cathode. The oxidation of the zinc in the one half-cell leads to an increasing concentration of the Zn^{2+} solution and a decreasing mass of the zinc electrode. In the other half-cell, the reduction of copper leads to a decreasing concentration of the Cu^{2+} solution and a mass growth of the copper electrode [34]. Materials like platinum or graphite permit electron migration without mass losses. To keep the reaction running, the solutions have to be kept electrically neutral. The overload of Zn^{2+} has to be compensated by positive ions that leave the half-cell, or negative ions have to be added. In the other half-cell, the reduction of Cu^{2+} ions in the solution means a deficit of positive charges in the solution. This has to be compensated by adding positive ions or removing negative ones.

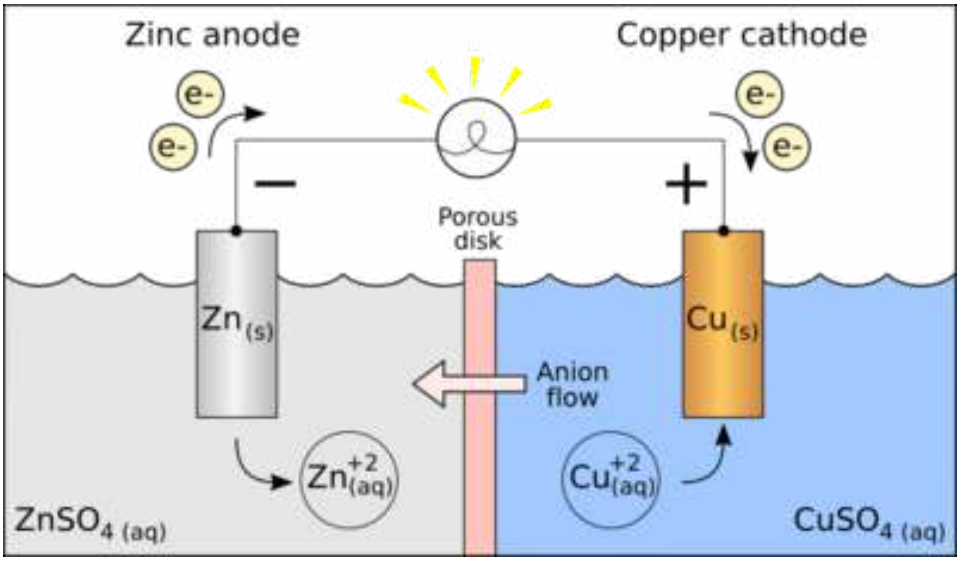

Figure 3.3.: Galvanic cell [35]

3.1.2. Effects on the environment

The dirt-battery is thought to be applied in a free-field scenario. The intention is, in the best case, just to put a piece of copper and a piece of zinc into the soil and start harvesting electrical energy.
In a society in which the ecological footprint is becoming a more and more important factor in making decisions for people in their buying-behaviour, as in times of decreasing availability of resources on one hand, but increasing demand for resources on the other hand, the question has to be asked how ecologically sense- or harmful a technology is.
An article by Greenpeace [36] calls attention to this topic, especially when copper is used. It is not broken down but stays in the soil and does harm the biodiversity. For example, the earthworm is banished by copper. In France In 1885 copper was becoming a common fungicide. Up to now it has been known as an almost perfect substance

for this application. Especially ecological wine farmers in the European Union are very dependent on the use of copper, since they are not allowed to use other fungicides. Mainly it is applied as copper-sulphate of which 3 kg/ha are allowed to be applied every year. In the 1960 of the last century, in some zones up to 60 kg/ha were applied annually.
The dirt-battery would leave zinc in the earth, while copper is brought from the soil to the copper electrode. That means, a dirt-battery could accumulate copper from a copper-polluted soil, lowering the copper-concentration in the contaminated soil.

3.1.3. Experiments

Figure 3.4.: The first earth-battery@19,9 kΩ

To start investigating the behaviour of an earth-battery, an empty bottle, made of Polyethylene Terephthalate (PET), cut at a height of 10 cm, some (old) flower soil, a piece of copper wire and a zinc-plated screw were used. Plugging just a multimeter in voltage mode resulted in a measured voltage of 0,81 V. Adding still mineral water did not really change anything, the voltage rose some tenths V but fell back after one or two minutes. Much more, moving of the parts in the soil changed the voltage.
Next, a load of a 19,9 kΩ resistor was applied to the dirt-battery. This action changed

the measurable voltage to about 0,4 V. As we know, Ohm's law is valid.

$$R = \left(\frac{U}{I}\right) \tag{3.1}$$

R	Impedance
U	Voltage
I	Current

Or, expressing the current:

$$I = \left(\frac{U}{R}\right) \tag{3.2}$$

This means that there is a current of 20 µA floating. Without touching anything, the voltage falls to 0,35 V after 3 h and then remains almost the same value. The used multimeter gives a value with 3 digits (definition 0.1-2.5% [37]). What was observed is that after turning off the multimeter for some hours, the voltage rises to about 0,37 V if measured again. It has to be supposed that the multimeter rises it's inner resistance when turned off. This is important, because in the dimensions of the measured values, always-present, parasitic effects as leakage currents are becoming important. Note that, in order to not disturb the circuit by moving the electrodes, the instrument was NOT disconnected, just turned off. Some current still has to be supposed through the multimeter when turned off. After floating the 17μA current for one week, the voltage never fell below 0,35 V but sometimes was almost 0,4 V.
Further tests of the dirt-battery cell showed that it is not a great effort to add fertilizers or salty water. Both just brought more voltage for a while (some hours) but after that period, the voltage was again about 0,3 V-0,4 V. What happens when changing the resistor of 19,9 kΩ to one of 22 Ω to test the high load case was interesting too. The Voltage decreased to 2 mV, which means that there now was a relatively high current of 90 µA floating. But: If you compare the two loads, in the 19,9 kΩ case, the multiplication

$$P = U \cdot I \tag{3.3}$$

gives a power of of 9,7 µW, with the 22 Ω resistor the power is just 0,18 µW. Another effect that was observed is that after two days running the current over the 22 Ω resistor, there was a notable corrosion on the zinc-screw as you can see in figure 3.5.

Figure 3.5.: Unused (left) and low-resistive load used (right) zinc-plated screw

At this point, it seems very reasonable to run the current over an impedance which is matched to the state (inner resistance) of the dirt-battery. The given problem is in a way similar to the one if using solar panels, since they neither have a constant output voltage depending on the load and the temperature, the maximum power can be reached by varying the connected load, so-called Maximum Power Point Tracking [38].
This first experiment helped to find structures for more investigations of the dirt-battery. It is obvious that a parallel set-up of dirt-battery cells should help to increase the output power because it is to expect that, by increasing the surface of the electrodes, the number of reactions and, thus, the number of electrons that can move increase. This is similar to an increase of current driven by the dirt-battery.

Figure 3.6.: A test device of a dirt-battery with fresh earth

By multiplying the surface of the electrodes, a rise of the output current is expected. It is supposed that the rise of current will not be linear to the multiplication of the surface, since in natural soil, many processes take place while running the battery (parasitic currents through the soil for example). In the case of the used zinc-screw, the surface calculated by

$$S_{\text{Screw}} = (2 \cdot r \cdot \pi \cdot l) \tag{3.4}$$

S_{Screw}	Surface of the screw
r_{Screw}	Radius of the screw ; $r_{\text{Screw}} = 5\,\text{mm}$
l_{Screw}	Length of the screw (covered by dirt); $l_{\text{Screw}} = 5\,\text{mm}$

gives a surface S_{Screw} of $157\,\text{mm}^2$. In the case of the multiplied surface by the test set-up shown in figure 3.6, the surface of the rectangular zinc-plated sheet of metal is

$$S_{\text{Plate}} = (2 \cdot a \cdot b) \tag{3.5}$$

where

S_{Plate}	Surface of the plate-electrode
a	width ; $a = 100mm$
b	height; $b = 80mm$

This gives a surface S_{Plate} of 1600 mm^2, thus, about 120 times the surface of the screw. The copper plate in this setup has the same surface as the zinc-electrode. If the current also rose by the same order, there would be an output of about 1200 µW. Unfortunately, as you can see in figure 3.7, these expectations are *not* fulfilled – the maximum output is about 400 µW.

Using a resistance decade, a sweep for different working points of the dirt-battery can be realized and the maximum power point can be found, else as the power that can be expected. There are probes for resistors ranging from 1 Ω to 100 kΩ with the set-up shown in figure 3.6. Note that this is a pseudo-logarithmic scaling of resistance. The difference between measured resistance values is 10 kΩ between 10 kΩ and 100 kΩ, 1 kΩ between 1 kΩ and 10 kΩ, 100 Ω between 100 Ω and 1 kΩ and so on. The data of the measurements can be found in table B.1. The used resistance decade is 1 W model from *breitbeil moser elektronik gmbh*. It was rent from the *Institut für Elektrische Anlagen* at the Technical University of Graz.

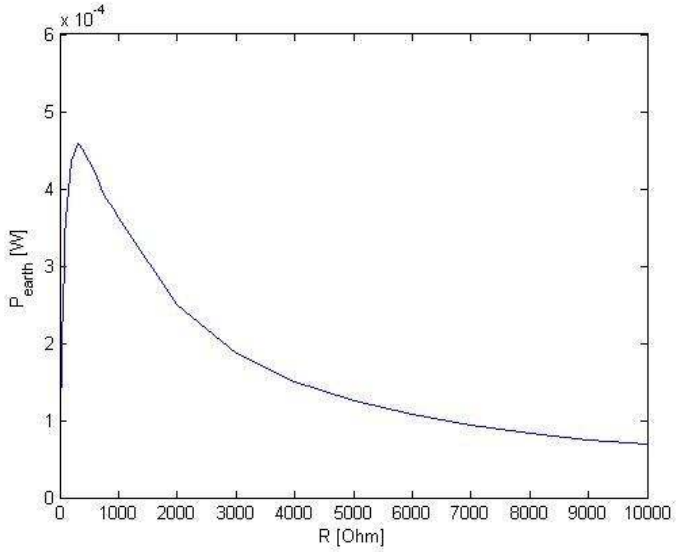

Figure 3.7.: Sweep over resistance loads applied to the dirt-battery

In figure 3.7, just resistors from 1 Ω to 10 kΩ are displayed, because there is very little current floating out of the dirt-battery above.

Obviously, a point exists where the power has a maximum. It is at a load with a resistor of 310 Ω, which drives a current of 1,2 mA. The measured voltage at this operation point is 0,377 V. The electrochemical effects which can explain this behaviour are very complex, especially because of the chaotic quality of usual soil in the sense of its chemical composition. It is not the intention of this work to be concerned with these questions, the behaviour of the dirt-battery is taken as a fact.
It is important to note that every tested dirt-battery increased its output power when the soil received some water, compared with the dry state. Furthermore, it was observed

that two weeks after connecting a 450 Ω resistor to this dirt-battery, a voltage of 370 mV still remained.

These observations were decisive to build a system which just works due to electricity generated by a dirt-battery. Because every flower can have 1 m^2-4 m^2 of meadow ground in the specific project at the *Skulpturenpark*, there is basically enough space to multiply the output of the source by putting many of these cells in serial/parallel constellations.

3.1.4. Theoretical consideration

The experiments described in section 3.1.3 showed, that the following equivalent circuit should be valid for the dirt-battery.

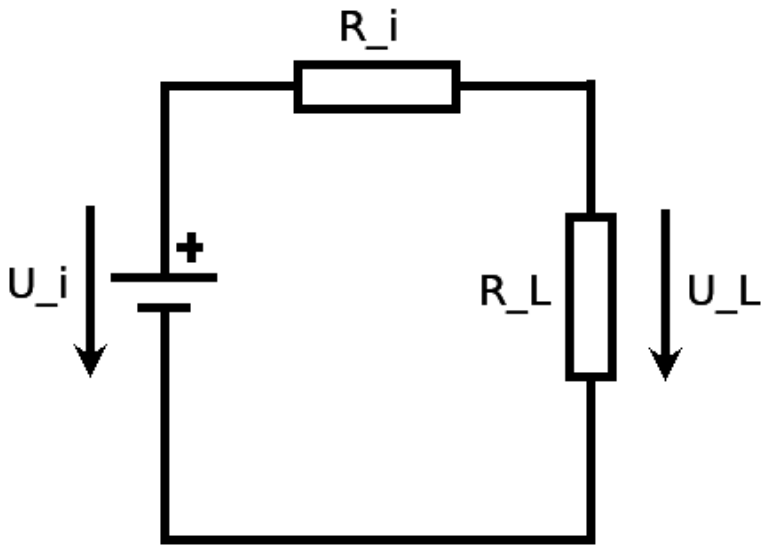

Figure 3.8.: Equivalent circuit of the dirt-battery

U_i	Cell voltage of the dirt-battery
U_L	Voltage at the connected load
R_i	Inner resistance of the dirt-battery
R_L	Resistance of the connected load

The power at the resistor is

$$P_\mathrm{L} = \frac{R_\mathrm{L}}{R_\mathrm{i} + R_\mathrm{L}} \cdot U_\mathrm{i} \cdot \frac{U_\mathrm{i}}{R_\mathrm{i} + R_\mathrm{L}} \tag{3.6}$$

P_L	Power at $\mathrm{R_L}$

$$P_\mathrm{L} = \frac{\mathrm{U_i}^2 \cdot R_\mathrm{L}}{(\mathrm{R_i}+\mathrm{R_L})^2} \cdot \frac{\frac{R_\mathrm{L}}{R_\mathrm{i}}}{(1+\frac{R_\mathrm{L}}{R_\mathrm{i}})^2} \tag{3.7}$$

$$P_\mathrm{L} = \frac{\mathrm{U_i}^2}{R_\mathrm{i}} \cdot \frac{\frac{R_\mathrm{L}}{R_\mathrm{i}}}{1+(\frac{R_\mathrm{L}}{R_\mathrm{i}})^2} \tag{3.8}$$

Equation 3.8 appears in an interesting form. The first term is a power that just depends on the cell voltage and the inner resistance of the source. It is definded as P_0.

$$P_0 = \frac{\mathrm{U_i}^2}{R_\mathrm{i}} \tag{3.9}$$

The second term just depends on the inner resistance and the load resistance. This term has the dimension [1], so it simply scales the first term. The aim is to chose a R_L that maximizes P_L.

If a relation

$$\frac{P_\mathrm{L}}{P_0} = \frac{\frac{R_\mathrm{L}}{R_\mathrm{i}}}{1+(\frac{R_\mathrm{L}}{R_\mathrm{i}})^2} \tag{3.10}$$

is expressed, the expression on the right is very significant, because it can be investigated easiliy.

This gets more obvious if

$$x = \frac{R_\mathrm{L}}{R_\mathrm{i}} \tag{3.11}$$

is chosen and the relation on the right side in equation 3.10 is substituted.

$$\frac{P_\mathrm{L}}{P_0} = \frac{x}{1+\mathrm{x}^2} \tag{3.12}$$

Now the relation $\frac{P_\mathrm{L}}{P_0}$ can be substituted by y and equation 3.12 is converted to

$$\frac{P_\mathrm{L}}{P_0} = y = \frac{x}{1+\mathrm{x}^2} \tag{3.13}$$

The envelope of y over values from 0 to 5 for x is shown in figure 3.9.

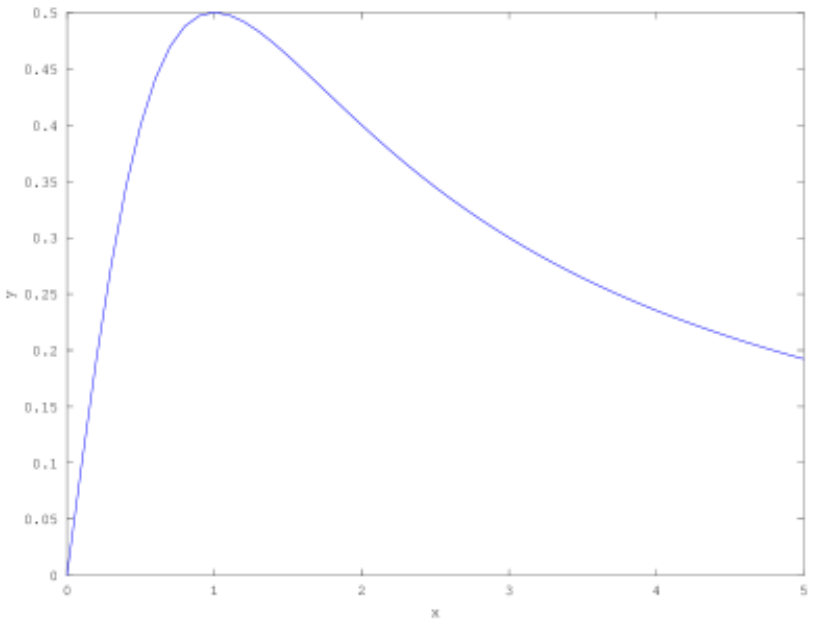

Figure 3.9.: Envelope of y over x

First, it is to note that the curve of y in figure 3.9 has a very similar shape to the one of the dirt-battery presented in figures 3.7 and 3.12. This means that the model describes the characteristics of a dirt-battery sufficiently.
It is easy to see that y has its maximum for $x = 1$ and that this maximum is 0,5. This can be demonstrated, when equation 3.13 is investigated:

$y(x = 0) = 0$
$y(x = \infty) = 0$

but, since y is not zero for all values of x, the extreme value of it is found by differentiation of equation 3.13.

$$y' = \frac{1 + \mathrm{x}^2 - x \cdot 2 \cdot x}{(1+\mathrm{x})^2} = \frac{1 - \mathrm{x}^2}{(1+\mathrm{x}^2)^2} \tag{3.14}$$

The maximum is where equation 3.14 gets 0, and that is for $x = 1$.

Exploiting equation 3.13 for $x = 1$ delivers $y(x = 1) = \frac{1}{2}$

With equation 3.11 follows that $\mathrm{R_L}$=$\mathrm{R_i}$ has to be valid for $x = 1$. This means that the inner resistance of the source has to be the same as the load resistance, if maximum output power is desired.

3.1.5. Practical application

For a particular application in a sound installation in the *Skulpturenpark* near to Graz, two dirt-batteries were built up and measured with a resistor decade as a load to the dirt-battery. The used batteries are shown in figure 3.10(a) and figure 3.10(b). The dirt battery in figure 3.10(a) is placed in a usual flower pot made of plastics.

(a) The small set-up with a diaphragm (SDN) (b) Big dirt-battery without diaphragm (BNNC)

Figure 3.10.: Two different set-ups of dirt-batteries

Figure 3.12 shows the measured power curves for loads between 1 Ω to 10 kΩ. The same pseudo-logarithmic resistor scaling, as mentioned in subsection 3.1.3, was chosen. For figure 3.12 and figure 3.11, the following indices are used for the 9 different set-ups:

- **BNNC:** big set-up, no diaphragm, no copper nitrate added, zinc centred
- **BNNL:** big set-up, no diaphragm, no copper nitrate added, zinc at the limit
- **BNCC:** big set-up, no diaphragm, copper nitrate added, zinc centred
- **BDCC:** big set-up, with diaphragm, copper nitrate added, zinc centred
- **BDNC:** big set-up, with diaphragm, no copper nitrate added, zinc centred
- **SNN:** small set-up, no diaphragm, no copper nitrate added
- **SDN:** small set-up, with diaphragm, no copper nitrate added
- **SNC:** small set-up, no diaphragm, copper nitrate added
- **SDC:** small set-up, with diaphragm, copper nitrate added

The big set-up is a bowl made of plastic with a volume of about 50 L. First, there is a copper shield with a size of 130 cm and 33 cm. Then the bowl is filled with soil. In the centre, there is a massive piece of zinc (BNNC set-up, see subsection 3.1.5). One

measurement series is also taken with the zinc piece quite close (5 cm) to the copper shield (set-up BNNL, see subsection 3.1.5). Because the output power was just reduced by the order of about 0,1 mW versus the case with the centred zinc piece, no more measurements were taken with this configuration. The small set-up is mainly achieved the same way, only that there is less earth between the zinc and copper electrode. The zinc electrode used in the small set-up is a zinc-plated screw with a diameter of 10 mm. Both set-ups are measured with and without the presence of a diaphragm.

The resistor decade was set to the corresponding value and connected to the output of the dirt-battery. Usually, without using a diaphragm, the measured voltage is not constant, but primly falling continuously to a value which seems *almost* stable. To realize the measurements, 5 s after connecting each resistor, the values were documented in table B.2. After this period of time, the measured voltage was almost stable. However, if one waited 1 min longer, this value would lower by a few mV. An important observation during the test period was that using a diaphragm in form of a flower pot made of porous clay, lowered the absolute value of output power, but the measured voltages at certain values of resistors appeared stable. That is the explanation why a version with a diaphragm should be favoured in an energy source application of the dirt-battery.

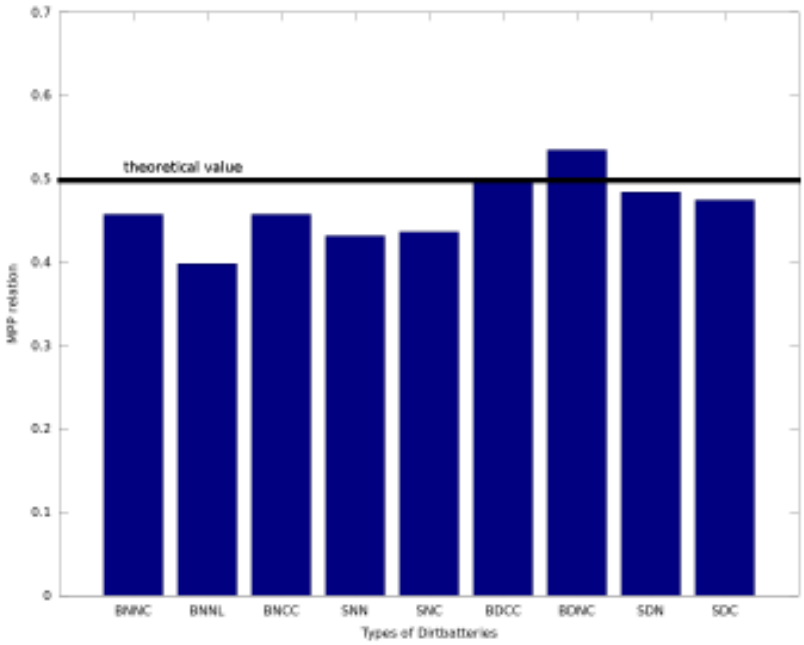

Figure 3.11.: The relation $V_{MPP}/V_{open\ circuit}$ depending on the set-up

V_{MPP} Output voltage of a source at its Maximum Power Point (MPP)

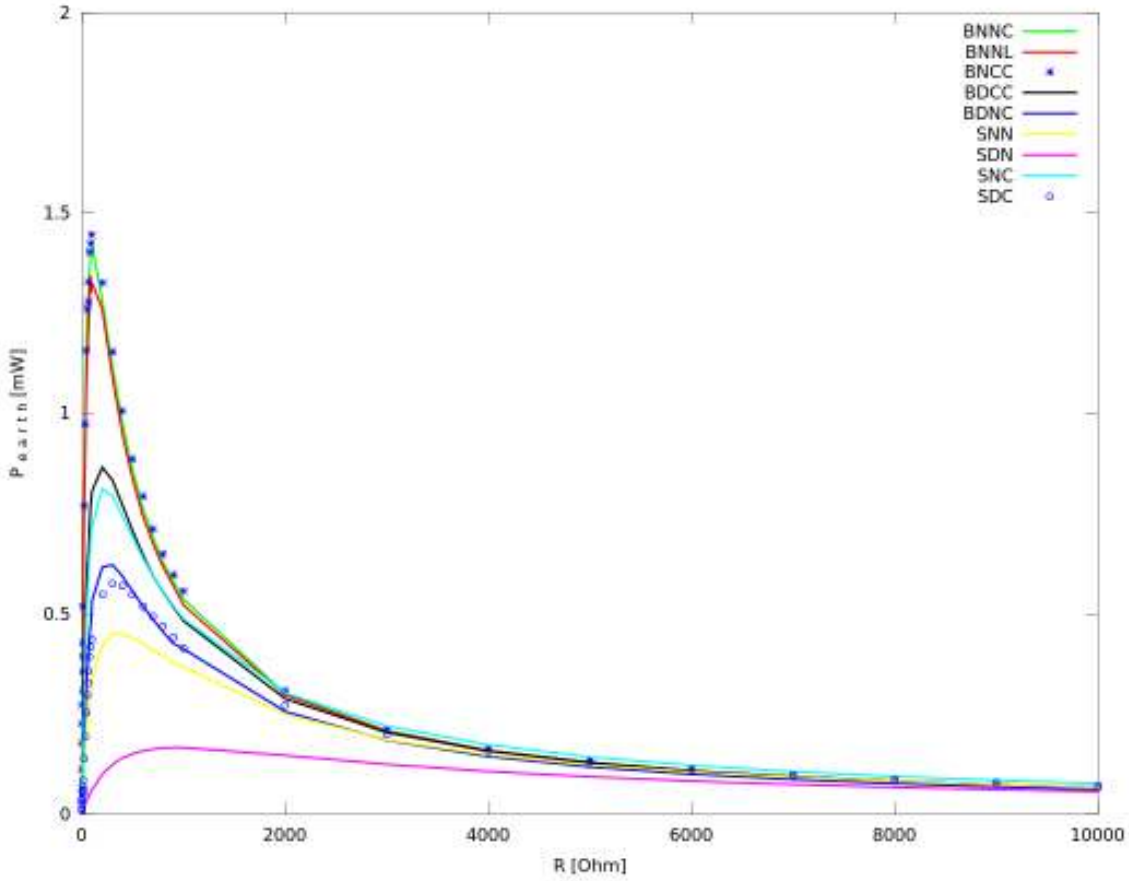

Figure 3.12.: Power curves depending on the set-up

Together with former knowledge of the dirt-battery, some conclusions can be drawn from this data. First, adding copper-nitrate does not seem to be a very effective way to tune up the dirt-battery. In the case of not using a diaphragm, the difference between using copper nitrate or not, is just about 0,1 mW. When using a diaphragm this value is about 0,2 mW.
It is very obvious that in all cases, using a diaphragm rises the value of the resistor as a load at which the output power reaches its maximum. It has to be supposed that a dirt-battery with a clay-pod diaphragm has a higher inner resistance than one without such a diaphragm. In figure 3.11 the points of maximum power, expressed by the relation $V_{MPP}/V_{open\ circuit}$ are displayed. These values are spread around 0,5, which is the theoretical value discussed in 3.1.4. This shows that the theoretical consideration coincidess quite well with the real dirt-battery.

The expected behaviour of the earth-battery output is similar to the one of solar panels, since both will mainly have DC output which varies by several parameters like sunlight,

temperature in the case of solar panels or the state of the electrodes, consistence and humidity of the soil in the case of the dirt-battery. The exact circumstances in a dirt battery should be investigated for future applications.

3.2. Photo Voltaic

Solar cells are already very common and have been used for many years [39]. A semiconductor is a material which increases conductance when it is exposed to light or heat [40] and decreases its conductance as it gets colder. The absorption of a photon by a semiconductor leads to a rise of the energy of an electron from the valence band to the conducting band. This happens when the energy of the photons absorbed by the material is higher than the band gap energy [41]. Since the electron is brought to the conducting band, it can move, which means that there can be a current. The effect of elevating electrons to the conducting band by absorbed light is called photo-effect and was discovered by *Alexander Bequerel* in 1839 [40].

Two of the three technologies for gaining electrical energy through solar panels are described in this work:

3.2.1. Silicon-based:

- **Wafer-based:** Those types have been the most used up to today and can be split into mono- and polycrystalline cells. The silicon basis material is doped, one side positive, the other one negative. This results in an electrical field, and electrons that get free to the conducting band caused by the energy of the absorbed light, are separated. A voltage is generated, and since there is an amount of electrons free to move, they will do so in the sense of a current through a connected resistor [40]. In figure 3.13, the layers of a typical crystalline silicon solar cell are shown. There is usually a cover glass that is held by a transparent adhesive mounted on the top. The anti-reflective coating helps preventing reflection of light, so that all the light reaches the semi-conducting layers. Those are held together with metal contacts. Crystalline-silicon solar panels have an efficiency of 15% to 25%. The technology nowadays can be considered reliable in many cases. There are devices working since the 1970s. The disadvantages of that principle is that crystalline silicon is a poor absorber of light and has to be relatively thick and rigid [39].

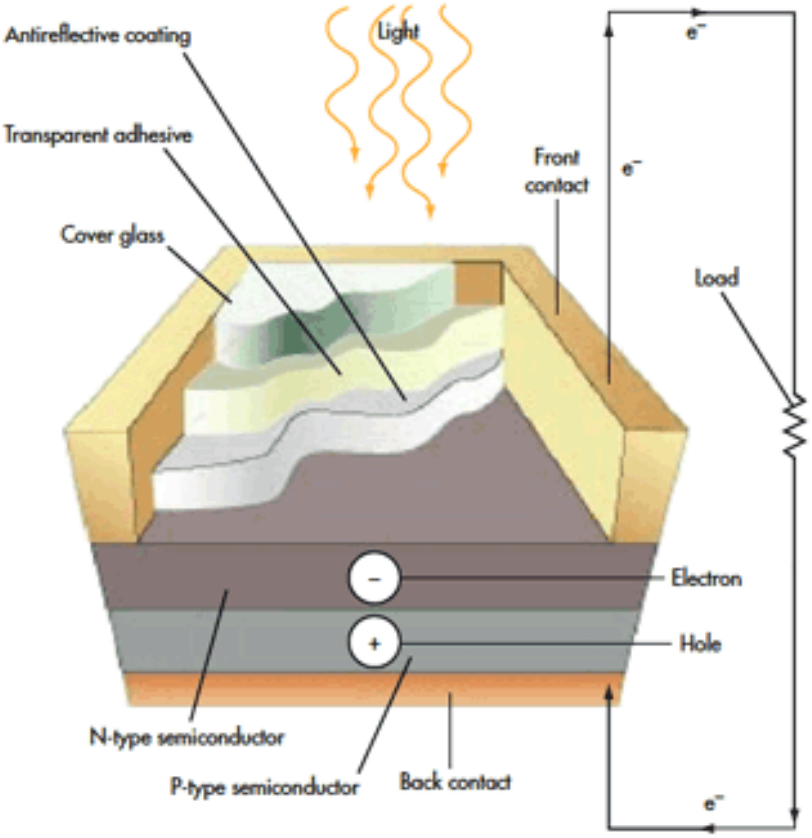

Figure 3.13.: Crystalline silicon Photo Voltaic (PV) cell [39]

- **Thin film:** A thin film of semi-conducting material is brought to a carrier like glass, plastic or metal by simple methods. This reduces costs and makes it worthy to develop the technology further. Up to now, they have been less efficient than crystalline versions. Since it is just a thin film, less material is necessary, and it is possible to produce flexible cells [42]. Thin-film solar cells can be grouped in four classical groups, depending on the material that is used. These are: amorphous silicon, thin-film silicon, copper indium gallium deselenide and dye-sensitized cells. Besides, there is organic material in use. As you can see in figure 3.14, the layer construction of these devices is very similar to the crystalline silicon technology. Instead of glass, a transparent coating is used on top. The principle of charge separation is the same in both cases. Differences compared to the crystalline silicon technology are the thin and flexible quality of thin-film solar cells as the different materials. Those are cadmium telluride and Copper Indium Gallium Deselenide (CIGS) instead of silicon.

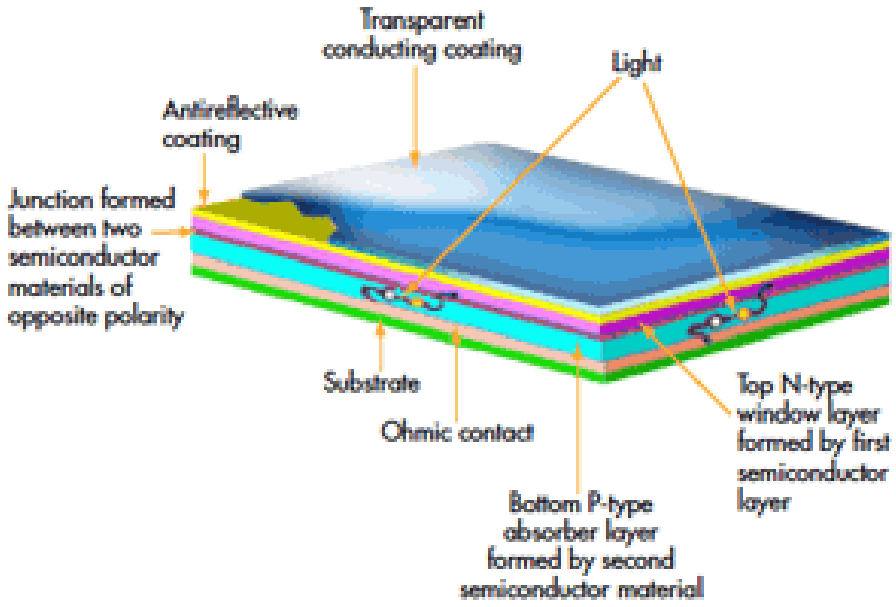

Figure 3.14.: Thin-film solar cell [39]

- **Triple Junction:** Triple Junction solar panels have three active layers. Each of them converts specific parts of the spectrum of the received light. The first layer – called the blue layer – converts Light with a wavelength between 300 nm to 600 nm. It is followed by the green layer (400 nm to 500 nm) and the red layer, which goes up to 1000 nm. This way, they achieve a higher efficiency factor at low solar radiation and under diffuse lights than crystalline cells.

  In the context of the phrase *energy harvesting*, the sunnyBAG® (shown in figure 3.15) is very interesting to mention. It is produced in Graz and equipped with a 1800 mAh lithium-ions accumulator and Maximum Power Point Tracking (MPPT). Triple-junction solar panels are used. The sunnyBAG® works with an efficiency factor of 9% [43].

Figure 3.15.: The sunnyBAG®[43]

3.2.2. Grätzel cell

Grätzel cells are working based on a non-galvanic chemical action. The active chemicals are permanently regenerated. They reflect green light and absorb red and blue light components. A sensitizer dye, that absorbs the red and the blue light, coats particles of titanium dioxide TiO_2. This configuration is placed between two electrodes in an electrolytic solution. This solution contains iodine ions.
When photons in the Ultra Violet (UV) or visible parts of the spectrum of light are absorbed by the TiO_2 combinations, they cause electrons to be injected into the conduction band of the TiO_2 and particles to move towards one of the electrodes. The Iodine ions collect electrons from the other electrode to regenerate the dye and establish a one-way current. It is cheap and easy to produce a Grätzel cell. They have lower efficiencies than common silicon-based cells (11% to 16%) [44].

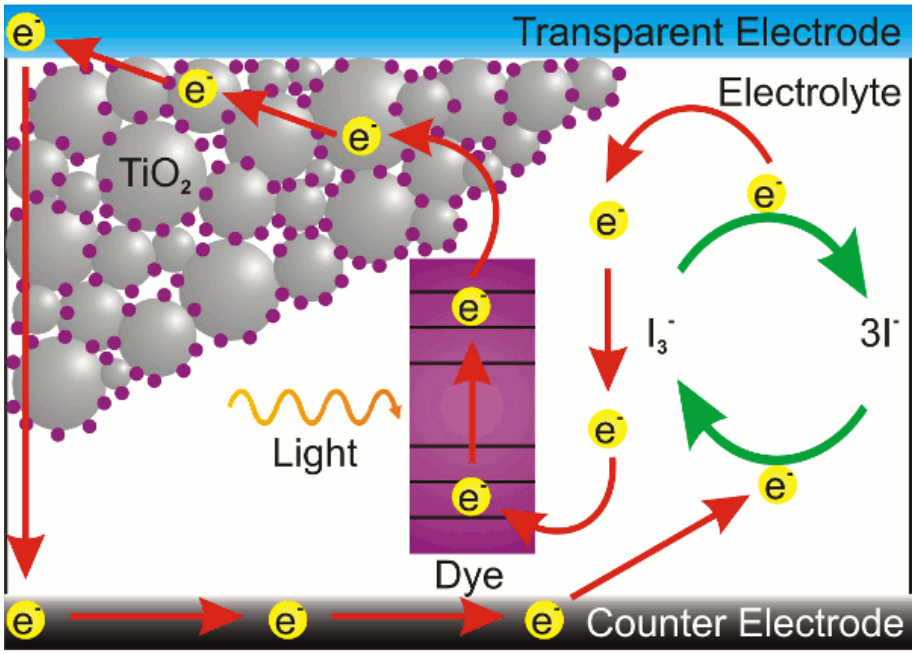

Figure 3.16.: Principle of a Grätzel cell [45]

As a sensitizer, dyes from flowers, leaves or fruits, which are the same as chlorophyll, can be used. *Dr. Robert Kartusch* from the University of Vienna published a guide for producing a low-cost Grätzel cell [46].

3.3. Thermoelectric Generator (TEG)

An electrical conductor that is heated at one end and cooled at the other one shows a temperature gradient. The *Thomson* effect explains the phenomena that in this case, there is a voltage difference between the cold and the hot end. *Thomas Johann Seebeck* discovered in 1841 that two wires, made of different metals and formed to a loop, show a voltage at the junctions if the temperature of them is different. Until the 1950s, this technology was investigated with different kinds of metals, but the efficiency just reached about 3%. Semiconductor-based thermal generators are able to achieve efficiencies of 5%, and the highest values ever measured were around 10%. As a conclusion, it can be declared that there are much more efficient methods of converting heat to electricity, than the presented technology. In many applications, the obtained amount of electricity can be very useful. Also *Kelvin* worked with thermoelectricity. He realized, that the voltage between the cold and the hot end of a wire is proportional to the temperature difference.

$$S = \frac{\Delta V}{\Delta T} \tag{3.15}$$

S	Seebeck coefficient [µV/K]
ΔV	Voltage between cold and hot end of the wire
ΔT	Temperature difference between cold and hot end of the wire

Two dissimilar material junctions are placed in the direction of a temperature gradient. With semi-conductor material, the achieved voltage is in the order of 100 µV/K to 300 µV/K. In semi-conductors, the kinetic energy of charge carriers depends more on the temperature than on the metals. For conductors, the *Seebeck* coefficient S is in order of a few µV/K. The *Seebeck* coefficient depends in a non-linear way on the material, the molecular structure and the absolute temperature. Because the measured voltage does not depend on the distribution of temperature in the conductor, but only on the temperature on the ends, the expression *temperature gradient* is often used. Other parameters of thermoelectric materials are the electrical connectivity σ, which should be high to minimize thermal losses, and the thermal conductivity λ. To maintain a high temperature Gradient between the two ends of the element, λ should be small.
Efficiency as an energy conversion element of a thermoelectric material can be expressed by the figure of merit Z.

$$Z = \frac{\sigma \cdot S^2}{\lambda} \tag{3.16}$$

Typically, heavily doped semi-conductors achieve the highest figure of merits, which traditionally is around one. Current developments achieve a value of four.

Presently, several junctions are connected in parallel or serial set-ups. An example of such a configuration is a thermopile [47]. It is shown in figure 3.17.

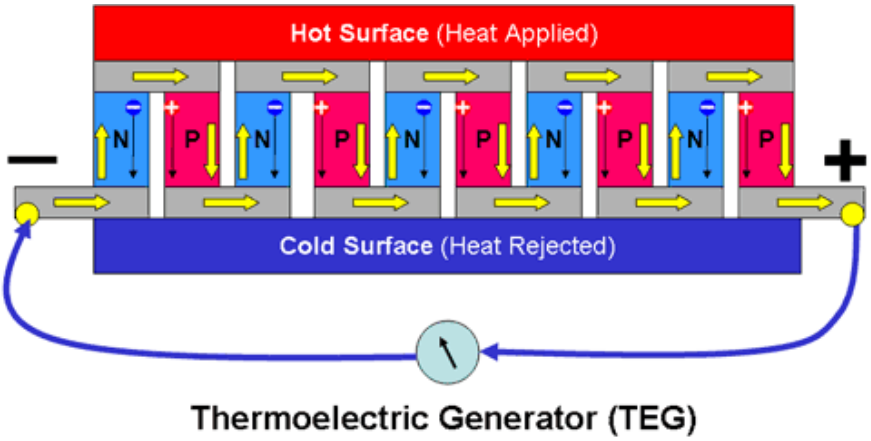

Figure 3.17.: Thermopile [47]

3.3.1. Thermoelectric Devices

Actually, because of the low electrical outputs, thermoelectric generators are just interesting for low power applications. On one hand higher temperatures are critical because of the robustness of the devices, and on the other hand, cooling the cold side often is very hard to achieve. In Radioisotope Thermoelectric Generators (RTGs), TEGs have been used as a portable power station in spacecraft applications. The heat is generated by the decay of radioactive isotopes like Plutonium 238 (Nuclear Batteries). Nowadays, applications in automotives are discovered in order to use some of the all-present heat wastes. 250 °C of exhaust gas temperature in combination with 50 °C of the cooling system could deliver 300 W in some experiments. Unfortunately, a rise of the coolant temperature to 90 °C means that the output power is divided by a factor of 2 [47].

- **Peltier effect thermo piles:** They are heat pumps that transport the heat from one side to the other. Efficiencies of 5% to 10% are possible. This fact makes them interesting just in cases with few space (mobile cooling) and, for example, to cool a Central Processing Unit (CPU) in a silent way because common compressor-based cooling systems can have an efficiency of 40% to 50%.
- **Seebeck effect thermo piles:** With them, it is possible to convert a temperature gradient to electrical energy. 1000 W of power is possible [47].

3.3.2. Applications

A very interesting project is presented on the web page of bioliteenergy [48].

Figure 3.18.: The use of the homestove in Ghana

By generating electrical energy with a TEG from of a wood fire, a ventilator is powered to optimize the burning of the fire. This leads to less air pollution. A Universal Serial Bus (USB) connector delivers electrical energy to charge a mobile device.

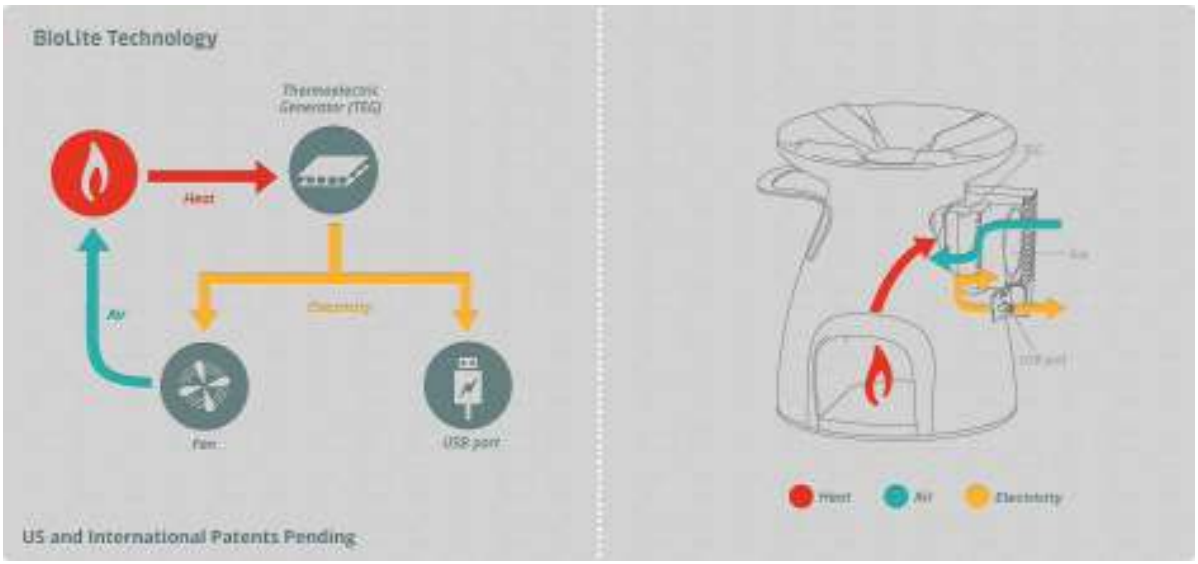

Figure 3.19.: The principle of the homestove

An interesting thermoelectric source is [49].

A guidance value for thermoelectric elements of 30 µW at a temperature difference of 5 °C for the watch *Thermic* by *Seiko* is mentioned [9].

3.4. Piezoelectric generators

Electrical energy is obtained by linear electromechanical interaction between the electrical and the mechanical state in a crystal. The piezo element is able to convert any mechanical energy, like vibrations, acoustic or impact triggered movements, like on a floor on which shoes have an impact. This technology can be exploited in a wide range of scales [11]. Piezoelectric energy harvesting of ambient vibration energy is probably able to deliver 10 µW up to some 100 µW of power. An efficient power interface, that extracts as much power as possible from the piezoelectric generator is necessary [50]. Therefore, mostly full-bridge rectifiers and voltage doublers are used. Together with the used power for control circuits of such devices, they limit the extractable power from a piezoelectric generator. The piezoelectric energy harvesting interface circuit presented in [50] uses a bias-flip rectifier. It is able to work at a power extraction capability that is four times greater than the one of full-bridge rectifiers. A typical device capable of gaining energy from a piezoelectric source, for example, is the *LTC® 3588-1* from *Linear Technology®* [51].

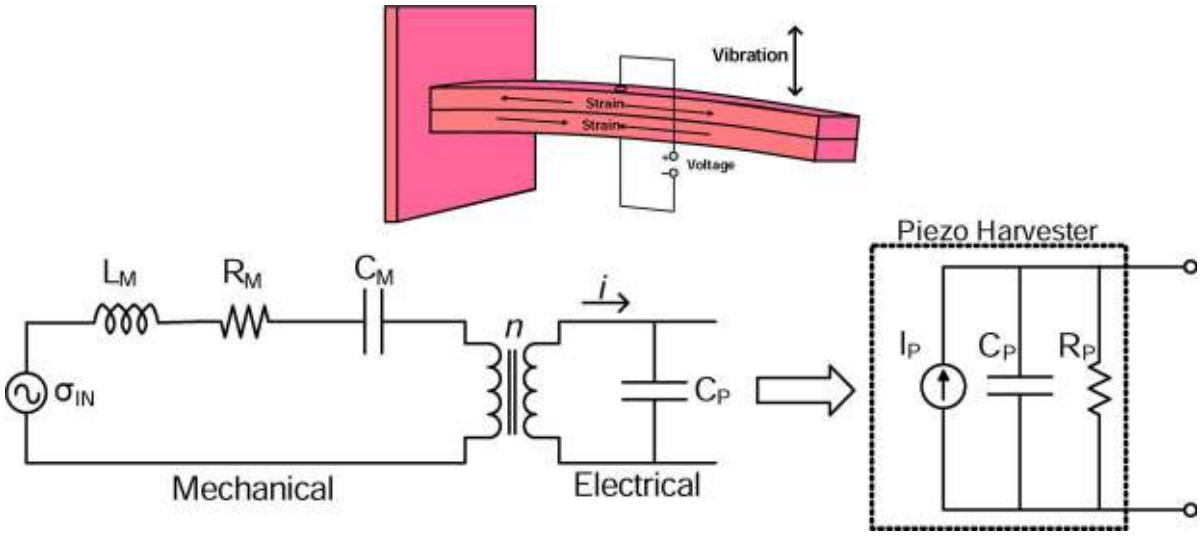

Figure 3.20.: Piezoelectric energy generator and equivalent circuit [50]

It is important to mention that there are applications for which damping of mechanical energy is desired. That means a win-win situation: On the one hand, damping is achieved, on the other hand, electrical energy is obtained.

3.5. Electromagnetic energy harvesting

It is a fascinating idea to gain electromagnetic energy which is just around, called *Ambient Radiation RF*, since there is a lot of discussion about *electric smog* and electromagnetic pollution. A technically educated person also might see the effect, that obviously and by the law of conservation of energy, the exploitation of this electromagnetic field must have an effect on this field, which means that it mainly must become damped. Again, it could be a win-win situation when the absorption of RF energy is desired.

3.6. Acoustic energy converter

A part of this work was done at the Instituto Universitario de Microelectrónica Aplicada de la Universidad de Las Palmas de Gran Canaria. Elisa Elías González did some experiments there with an *Advanced Linear Devices EH300 energy harvesting module* to harvest the energy converted by a conventional loudspeaker in a sound field [9]. It was possible to receive an energy output of 4.6 mJ at 3.6 V in about 3 min when the sound source (same model of loudspeaker like the receiving loudspeaker, 110.6 dB) was at a distance of 4 cm. For the discussed application, this is not an option because of the high price of the *EH300* (about €40 Mouser, 25.11.2012). The great advantage of this converter is that it works with DC as well as with AC sources.
The results of the investigations done in the project *Diseño de un sistema de captaciòn de energìa residual basado en al acondicionador EH300 de la empresa ADVANCED LINEAR DEVICES* at the Universidad de Las Palmas de Gran Canaria show that it is possible with the EH300, a loudspeaker and a transformer, to run a low-power electronic device like the PFB. The *EH300* is able to convert AC input signals to a DC voltage of a programmable value and store it to a storage element like a capacitor or a battery. A vision is, that the leaves of the flower are moved by the wind, agitating a magnet in a coil and by this, inducing voltage in the coil. This voltage is converted by the *EH300*. The strongest argument against using this technique is the price which is about the tenth using a DC source with an adequate interface like the *bq25504* presented in chapter 4.1.

4. Power Management

To run a unique cell of dirt-battery (without connecting several cells in series), the power out of it has to be extracted at a high efficiency. A dirt-battery, at its MPP, has a voltage of about 0,4 V, too little to run any electronic device. Thus, a conversion of this DC voltage to higher values (for example 3,3 V in many cases) has to take place like a storage at this voltage in a battery or supercap.
All this is also valid for photo-voltaic and thermoelectric generators when just a few cells are used.

4.1. Texas Instruments bq25504

The device was elected to be one of the 2011 *Product of the Year Award* winners by the *Hearst Electronic Magazine* [52]. It is capable of interfacing to the output of the dirt-battery to load a capacitor, super cap or thin film battery to an adequate voltage. The Maximum Power Point (MPP) (see also chapter 4.1.2) can be set by a resistor divider or alternatively by a reference voltage which is prepared by the micro-controller. This allows more complex algorithms to catch the MPP when using a source with a time-varying behaviour. Actually, the relation of the open-circuit voltage to the voltage of Maximum Power Point (MPP) is set up. The experiments made with dirt-batteries explained in subsection 3.1.3 showed that this relation is quite depending on whether an additional diaphragm is used or not. Hence, from the current point of view, it is not necessary to implement the mentioned dynamic set-up of the MPPT based on a reference voltage generated by the micro-controller.

The operation of the boost converter starts when there is enough voltage on the input pin (VIN_DC) or from the battery pin (VIN_BAT) to raise the voltage on VSTOR above 1,8 V. Below this value on VSTOR, the cold-start subsystem of the circuit is activated.

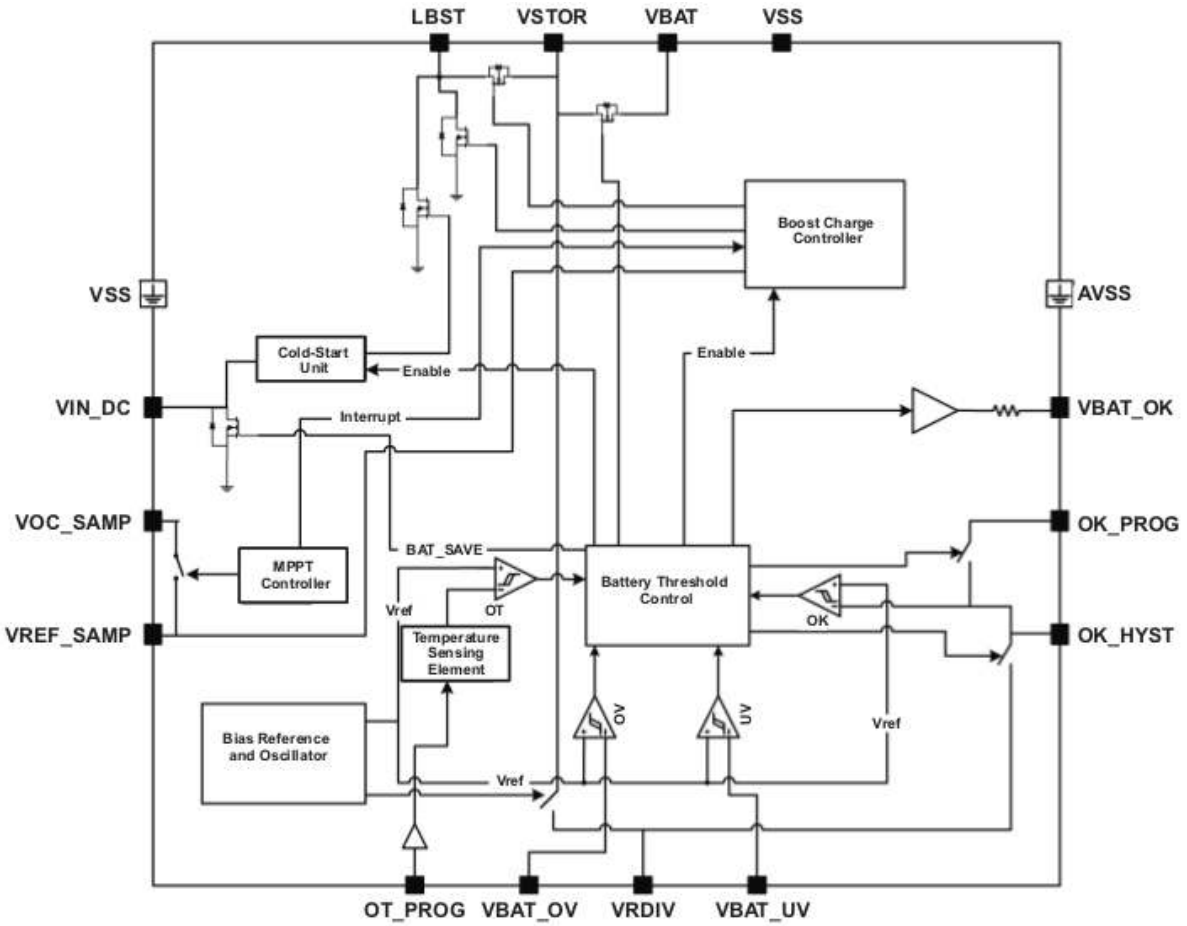

Figure 4.1.: bq25504 high-level function diagram [53]

4.1.1. Boost Converter

The main work of the *bq25504*, besides the management of the storage element, is to raise the value of the output voltage of the earth battery to a value which allows operating a micro-controller and peripherals. The voltage conversion is done in a very economic way by a boost converter [54]. Figure 4.2 shows the principle of a boost converter. The storage phase is initiated by closing the switch. A current which increases according to the time constant of the circuit is driven through the inductor. Opening the switch lets the voltage increase across the switch because the collapsing magnetic field of the inductor intends keeping the current. When the voltage increases, the diode becomes conducting. This period in which the diode is conducting and therefore the capacitor is loaded is called *delivery phase*. It ends, when the energy stored in the inductor is too little to make the diode conducting [55].

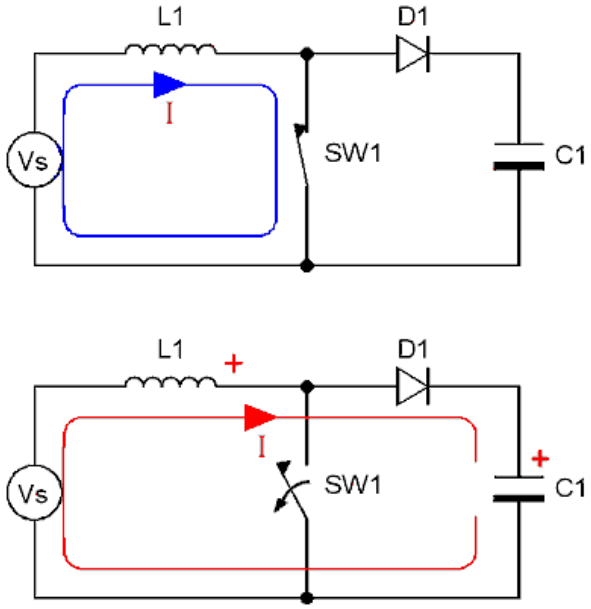

Figure 4.2.: Principle of a boost converter [55]

The boost converter in the *bq25504* needs a voltage of more than 1,8 V at the VSTOR pin to start an operation. This voltage can come from the VIN_DC input pin or from a battery or capacitor connected to the VBAT pin. If the voltage at VSTOR is less than 1.8 V, the cold-start sub-system is used to get the boost converter started. Between the energy storage capacitor VSTOR and the battery, there is a P-Channel Metal-Oxide Semiconductor (PMOS) switch. In the case that a battery (or capacitor) is connected to the VBAT pin, the PMOS switch is closed, so that the VSTOR capacitor can be loaded by the battery (if energy is available from it). If there is not enough energy stored in the battery or capacitor to rise the voltage of the VSTOR capacitor above 1.8 V, the PMOS switch is opened again (after 20 ms) and the cold-start sequence is started. It needs a minimum of 330 mV to start extracting energy from the source. Once running, voltages down to 80 mV can be processed. The cold start system is less efficient than the boost converter but the device can stay in this mode during operation. It is important to keep in mind that a characteristic of a boost converter is that a voltage at the input of the converter which is higher than the voltage of the battery is brought directly to the output.

4.1.2. Maximum Power Point Tracking

This is a common technique to adapt the load connected to the output of a DC source, mainly of photo-voltaic cells, since they have a non-linear output efficiency depending on light, temperature and total resistance. The observations on the dirt-battery showed that this source also has a Maximum Power Point (MPP). Depending on the load you connect

to the battery, the product $U \cdot I$ has a maximum. From this point of view, it makes a lot of sense to use a DC/DC converter which can vary this resistance or impedance. This leads to a load which is fitted to the circumstances (for example, the state of the used dirt-battery, depending on the corrosion of the metals like the concentration of electrolyte and copper-nitrate) to have the highest possible output power. For solar cells, this typically is about 80% of their open circuit voltage [53].
The *bq25504* has an input pin (pin VREF SAMP) to programme the input voltage at which the source is driven as a percentage of the open-circuit voltage. The inner effective impedance which is modulated by the boost converter in order to extract as much power as possible (MPPT) can be programmed in relation to the open-circuit voltage of the source, following the formula

$$VREF\_SAMP = VIN_{\mathrm{DC}}(OpenCircuit)\left(\frac{R_{\mathrm{OC1}}}{R_{\mathrm{OC1}} + R_{\mathrm{OC2}}}\right) [53] \tag{4.1}$$

$VREF\_SAMP$ The voltage at which the source has its MPP for a given open-circuit voltage
$R_{\mathrm{OC1}}, R_{\mathrm{OC2}}$ Resistors to programme $VREF\_SAMP$

$$\frac{VREF\_SAMP}{VIN_{\mathrm{DC}}(OpenCircuit)} = \left(\frac{R_{\mathrm{OC1}}}{R_{\mathrm{OC1}} + R_{\mathrm{OC2}}}\right) \tag{4.2}$$

The MPP of the dirt-battery prototype shown in figure 3.6 was found at a voltage of 0,37 V, while the open loop voltage was 0,87 V. Besides, the data sheet of the *bq25504* [53] suggests obtaining a sum of $R_{\mathrm{OC1}} + R_{\mathrm{OC2}} = 20\,\mathrm{M\Omega}$. That means, R_{OC1} should be 8,52 MΩ and R_{OC2} 11,48 MΩ.
Because not all values of resistors are available, it has to be decided whether if it is more worthy to take the next higher or the next smaller value for the resistors. As you can see in equation (4.2), when R_{OC1} becomes higher, with fixed values for R_{OC2} and $\mathrm{VIN_{DC}}$(Open Circuit), $VREF\_SAMP$ becomes larger, while an enlargement of R_{OC2} provides a smaller value for $VREF\_SAMP$. By contrast, for a good performance, the sum of the two resistors should differ as little as possible from 20 MΩ. Also, it is important to keep in mind figure 3.7, which shows a definitive point of maximum power of the dirt-battery. On the x-axis in figure 3.7, there is the resistive load in [Ω]. The voltage on the dirt-battery increases with this resistance. The curve shows that it is more likely to reach the MPP (or getting close to it) choosing a value for $VREF\_SAMP$, that is slightly higher than the desired $VREF\_SAMP$ (in figure 3.7, this means a higher resistance as a load). Hence, R_{OC1} to 8,45 MΩ and R_{OC2} to 11 MΩ seem to be a smart solution. This choice gives a sum of the two resistors R_{OC1} and R_{OC2}, which is about 0,5 MΩ less than the suggested sum, yet, this is just an error of 2,25%. This set-up tunes the $VREF\_SAMP$ to 3,77 V. This is quite close to the measured Maximum Power Point (MPP) of the dirt-battery.

As it can be seen in figure 3.11, using a diaphragm, which is recommendable in order to prohibit unwanted and parasitic currents through the soil, rises the voltage relation expressed in equation 4.2 to about 0,5 or even a bit higher in the case that no copper nitrate is used. Because of the narrow zone of relatively high output power of the dirt-battery seen in figure 3.12, R_{OC1} and R_{OC2} have to be changed to reach the point of maximum power. To fulfill a relation mentioned in equation 4.2 of 0,5 $R_{\mathrm{OC1}} = R_{\mathrm{OC2}} = 10\,\mathrm{M\Omega}$.

The *bq25504* includes a battery management system. R_{index} are the resistors which have to be dimensioned to programme the device. V_BIAS is the reference voltage, internally generated and used by the *bq25504* to set thresholds. It is obligatory to programme the following three values for extracting energy of the source (formulas taken from [53]).

4.1.3. Battery Voltage Range

This setting sets the minimum-maximum range of the voltage in the storage element. As long as there is enough energy from the source but no over-voltage, the voltage in the storage element will be kept within the programmed limits by the *bq25504*.

- **Battery Under-Voltage Protection**
  This function of the *bq25504* is thought to prevent rechargeable batteries from deep discharging. In the here presented work, further the micro-controller, even in sleep mode, needs at least 1,8 V because the RTCC has to keep running, otherwise synchronization with the other PFBs would be lost. The *MRF89XAM8A* has a minimum operating voltage of 2,1 V. VBAT_UV is the threshold voltage when the battery voltage decreases from a higher voltage. It prohibits further discharge than this value. Of course, this is just possible while there is enough power from the source to compensate losses and the consumption of the RTCC. To have some overhead, 2,2 V was considered for $VBAT\_UV$.

$$VBAT\_UV = VBIAS\left(1 + \frac{R_{\mathrm{UV2}}}{R_{\mathrm{UV1}}}\right) \text{[53]} \tag{4.3}$$

  To ensure that the storage element is not discharged much lower than to 2,2 V, the smallest V_BIAS mentioned in the data sheet [53], which is 1,21 V, is taken.

$$2,2 = 1,21\left(1 + \frac{R_{\mathrm{UV2}}}{R_{\mathrm{UV1}}}\right) \tag{4.4}$$

  Further, the data sheet says that $R_{\mathrm{UV1}} + R_{\mathrm{UV2}} = 10\,\mathrm{M\Omega}$, so we need a $R_{\mathrm{UV1}} = 5{,}5\,\mathrm{M\Omega}$ and a $R_{\mathrm{UV2}} = 4{,}5\,\mathrm{M\Omega}$. Because of availability, $R_{\mathrm{UV1}} = 5{,}49\,\mathrm{M\Omega}$ and a $R_{\mathrm{UV2}} = 4{,}53\,\mathrm{M\Omega}$ resistors are mounted on the PFB board. This provides an even

higher voltage level, which now is 2,208 V.

- **Battery Over-Voltage Protection**
  This value determines the over-voltage threshold for the battery/supercap. The device will not be loaded to a higher voltage. The supercap mounted on the PFB prototype has a maximum voltage of 4,2 V, but it has to be kept in mind that the maximum voltage of the *PIC16LF1823* and the *MRF89XAM8A* is 3,6 V. That is why this value has to be used for VBAT_OV, which is the pin of the *bq25504* that permits programming the upper limit of the voltage in the storage element.

$$VBAT\_OV = \frac{3}{2} VBIAS \left(1 + \frac{R_{\mathrm{OV2}}}{R_{\mathrm{OV1}}}\right) [53] \tag{4.5}$$

  To always guarantee that no higher voltage than 3.6 V appears as a supply voltage in the system, VBIAS was assumed with its maximum value, 1,27 V.
  This and the fact that $R_{\mathrm{OV2}} + R_{\mathrm{OV1}} = 10\,\mathrm{M\Omega}$ is demanded in the data sheet [53], leads to $R_{\mathrm{OV1}} = 5{,}29\,\mathrm{M\Omega}$ and $R_{\mathrm{OV2}} = 4{,}71\,\mathrm{M\Omega}$ as solutions. Finally, $R_{\mathrm{OV1}} = 5{,}36\,\mathrm{M\Omega}$ and $R_{\mathrm{OV2}} = 4{,}75\,\mathrm{M\Omega}$ are available, which sets up a VBAT_OV of 3,59 V.

4.1.4. Thermal Protection

The device offers the possibility of thermal shut-down, either it turns off at 65 °C, if the OT_PROG pin is tied low, or at 120 °C, if this pin is tied high. The PFB uses a supercap with an operating temperature range of -40 °C to 70 °C, so the thermal shut-down should happen when the temperature exceeds 65 °C, or in other words: Pin 5 has to be grounded. Because of the flexible layout of the PFB, a resistor with 0 Ω has to be mounted in order to ground the pin properly. The *bq25504* is turned to a stand-by state when an over-temperature event occurs and remains there until the temperature falls below the limit again. A hysteresis of about 5 °C is realized [53].

4.1.5. Battery Voltage in Operating Range

The device signals a voltage of the storage element in a programmable operating range. While the voltage of the storage element is in this range, VBAT_OK is set to VSTOR, which also is the supply voltage for the whole circuit. When the battery voltage is increasing from, let us assume 0,5 V, the VBAT_OK pin gets high at the value to which VBAT_OK_HYST is tuned to. It is tried to store as much energy as possible in the supercap, but reaching VBAT_OK_HYST has to happen before the VBAT_OV in every case. Reaching VBAT_OV before setting VBAT_OK would lead to a state in which the VBAT_OK pin is never high and the PFB is never signalized that there is sufficient energy to act. VBAT_OK_HYST is chosen to be 3,5 V. Looking for the worst case,

which means loading the storage element to the upper limit of the circuit, the maximum value for V_BIAS is chosen. It is 1,27 V.

$$VBAT\_OK\_HYST = VBIAS\left(1 + \frac{R_{OK2} + R_{OK3}}{R_{OK1}}\right) [53] \tag{4.6}$$

For a decreasing battery voltage, the VBAT_OK pin will be 0 (0 V) when the voltage of the storage element becomes less than the value VBAT_OK_PROG is set to. This value should always be above 1,8 V, that is the minimum voltage to run the PIC16LF1823. To still have some overhead, the VBAT_OK_PROG level is tuned to 2,5 V. The aim is that the micro-controller, after recognizing the change of VBAT_OK, has some spare energy to terminate calculating, saving and/or sending actions.

Also, to ensure a worst-case function stability, this calculation is done applying the minimum V_BIAS, which is 1,21 V.

$$VBAT\_OK\_PROG = VBIAS\left(1 + \frac{R_{OK2}}{R_{OK1}}\right) \tag{4.7}$$

These have been two equations so far and three variables. The third equation is delivered by the data sheet [53].

$$R_{OK1} + R_{OK2} + R_{OK3} = 10\,\text{M}\Omega \tag{4.8}$$

And the results are: $R_{OK1} = 3{,}63\,\text{M}\Omega$, $R_{OK2} = 3{,}87\,\text{M}\Omega$, $R_{OK3} = 2{,}5\,\text{M}\Omega$.

4.1.6. Inductance

The data sheet of the *bq25504* says, an inductance with a value of 22 µH should be used for L1 in the circuit presented in figure C.1 and for L_BST1 shown in figure C.5. It should have a maximum series conductance to keep high efficiency and extend at least peak currents of $\geq 250\,\text{mA}$. Obviously, the *Coilcraft LPS4018-223MLB* coil, which is mounted on the *bq25504 EVM* board, works quite well. But because it is difficult to order the *Coilcraft* coil in small amounts (extra shipping costs of €40,- to Austria), at first a *Murata LQH32CN220K53* coil was soldered on the first prototypes. As suggested by the data sheet of the energy harvesting chip, the inductance value was 22 µH, but the serial resistance of this coil is 0.71 Ω and the serial resistance of the *Coilcraft LPS4018-223MLB* is just 0,36 Ω. Unfortunately, this alternative coil does not work properly, meaning that the prototype of the PFB ver. 0.1 was not able to rise the voltage of the capacitor higher than the input voltage. Inserting the coil from the evaluation board into the prototye made the prototype work.

4.2. Power storage

The output voltage of the dirt-battery needs to be converted to obtain a voltage of at least 2.1 V to run the *MRF89XAM8A* transmitter, which is the most energy-intensive part the electrical circuit of the PFB and also needs the highest minimum voltage. The advantage of using a super capacitor is that this type of storage can be charged and discharged very quickly [56]. The qualities of some possible storages are evaluated, and by estimating the size necessary, a fitting technology is chosen.

4.3. Low-Voltage Boost Converter Module

With new Low-Voltage Booster Modules (LVBMs), it is possible to boost the low voltage output of a low power energy source to a voltage, which can start an energy harvesting module like the *bq25504*. This is very useful when you have to expect times without any input voltage. Because of the losses, it is not possible that the system maintains the charged capacitor for a very long time. To get the boost-converter of the *bq25504* started, 1,8 V are necessary, see also section 4.1. The dirt-battery will not lose its power suddenly, but it will become weaker as the zinc-electrode disappears or the chemical concentration of elements necessary for the redox-reaction becomes lower. While the *bq25504* does not get below the VBAT_UV value, the boost charger keeps running. Because the dirt-battery has a quite slow behaviour, software detection of losing energy is possible by measuring the time between VBAT_OK events.

5. Micro-controller – Microchip PIC®16LF1823

This chip offers very low power consumption. Unfortunately, it was found out that its pin count is not sufficient for debugging with the *MRF89XAM8A* low-power RF module because not all pins necessary can be connected to the micro-controller. It can be deployed in a later step when no debugging is necessary. The *PIC® 16LF1826* has 18 pins, so it is enough to have extra connections for programming and debugging. Its current consumption @1 MHz is twice the one of the smaller controller. In sleep mode, the *PICLF1823* consumes 20 nA, while the *PIC® 16LF1826* consumes 30 nA. Because of the different pinning, it cannot be mounted directly to the current PCB board of the PFB ver. 0.1. A possibility for debugging is to use a PFB just for the output of received signals. Then, the CS_Data pin does not have to be used and the CS_Config pin can temporarily be connected to the pin 7 of the *PIC® 16LF1823*. For the interrupt, it actually has to be connected to the INT pin of the micro-controller. A solution could be to use the INT pin with the VBAT_OK pin of the bq25504 in parallel with the IRQ0 pin of the *MRF89XAM8A*.

5.1. Low Power in terms of Processing

Since micro-controllers nowadays usually are kinds of CMOS devices, the power consumption can be split up in two types of consumption: dynamic power, which appears, when the device is running the program, while static power refers to the consumption when the device is not working but connected to the supply voltage [57].

- **Dynamic power consumption:** In a Complementary Metal Oxide Semiconductor (CMOS) Inverter, there are very low currents when the input is at the value of the negative supply voltage (VSS) or the positive supply voltage (VDD). During the change from one of these states to the other, higher currents which are significant in terms of low power appear. Also load capacitance which in a real system always appears, is notable, since it has to be loaded and unloaded every time the voltage switches. For a CMOS device, the dynamic power consumption can be calculated the following way

$$P = U^2 \times f \times C \tag{5.1}$$

P	Dynamic power
U	Voltage
f	Frequency
C	Current

In this equation, it becomes very clear that voltage is the most important factor to minimize the power consumption in a CMOS device because the value of voltage is squared.

- **Static power consumption:** Static power is the power necessary for maintaining proper system operation without running code. This refers to bias currents in analogue circuits, low-power time keeping oscillators (see section 5.2) and leakage currents [57].

First, there was the idea to use the *PIC® 16f639*, which includes an analogue front end that can be used for a 3-channel 125kHz bidirectional transponder communication (Low Frequency (LF) talk back) [58]. The LF talk back means that this chip is able to communicate with a base station LF transmitter/receiver by modulating the received RF signal. This is done by 3 antennas (one for each direction, and they are connected to the pins 9-11 of the controller). Each of these 3 pins represents a modulation circuit. There is a modulation transistor (Field-Effect Transistor (FET)), internal tuning capacitors and external Inductance (L) and Capacitance (C) antenna components. The modulation transistor and the internal tuning capacitors are connected between the LC input pin and the LCCOM pin of the micro-controller. Each LC input has its own modulation transistor. When the modulation transistor is turned on, its low turn-on Resistance (R_{M}) clamps the induced LC antenna voltage. The coil voltage is minimized when the modulation transistor is turned on and maximized when the modulation transistor is turned off. The modulation transistor's low turn-on resistance (R_{M}) results in a high modulation depth [58]. This is a very energy-efficient way to communicate on short distances and often used for key-less entry applications. But this technology is not suitable for the project in this thesis because every single system should be able to send and receive data by RF. After some research based on this knowledge and the former decision to choose a controller of *Micrchip* PIC®s, it was decided to use the *PIC® 16F1823*. It consumes very little power compared with other low power micro-controllers. This is due to the fact that it represents a quite minimalistic solution. Since it communicates with the RF-module via SPI and General Purpose In-/Outputs (GPIOs), it can be replaced in an easy way in future revisions of the PFB circuit by more complex micro-controllers.

Features:

- 14-Pin Flash micro-controller with nanoWatt Extreme Low Power (XLP) Technology
- operating voltage range 1,8 V-3,6 V
- standby current typical 20 nA@1,8 V
- operating current 34 µA@1 MHz, 1,8 V; typical
- SPI interface
- Real Time Clock and Calender (RTCC)

5.2. Real Time Clock and Calender (RTCC)

To enable the network to be very energy-efficient, the units have to be synchronized. They should be in a sleep mode most of the time, and, at defined time slots, they have to wake up, communicate with their neighbours, save data, maybe ring the bell and sleep again.
A common method to solute tasks like this is to implement a RTCC, for which the *PIC® 16LF1823* is well prepared, since it supports running the external crystal oscillator at a low frequency of 32.768 kHz. The RTCC concept is to run the oscillator in sleep mode and after a certain period of time wake it up, increment a counter, put the device in sleep mode again in which it continues oscillating. Based on the obtained time data, it acts at certain time slots. It is supposed that all of the PFBs in a swarm are exposed to the same temperature, so no special care is taken concerning temperature compensation of the crystal oscillator.

5.2.1. Crystal operation

Between the OSC1 and the OSC2 pin of the micro-controller, a quartz crystal can be connected as shown in the following scheme

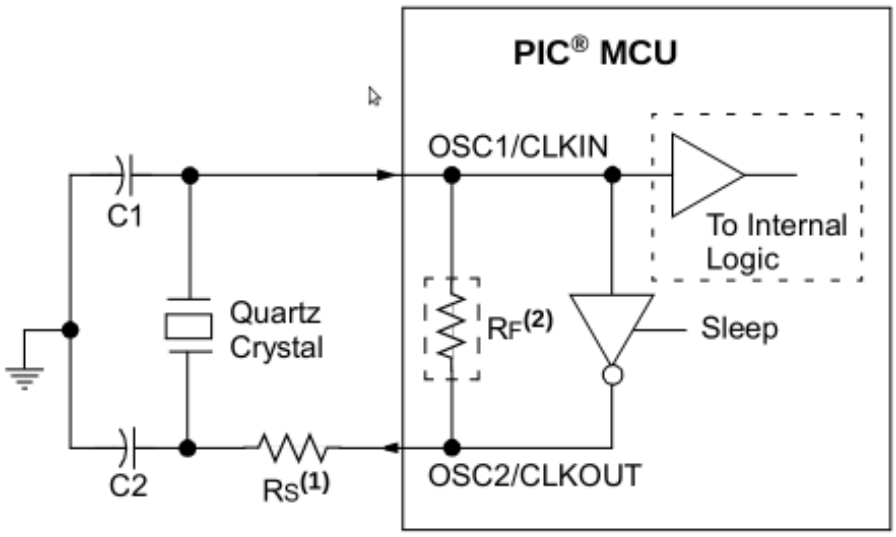

Figure 5.1.: Quartz crystal oscillator mode [4]

There is further support by *Microchip*® to obtain the values of C_1 and C_2, which are suggested to be chosen equally in [59]. This paper claims that the *PICmicro*® devices are equipped with a pierce oscillator for which the equation is

$$C_{\mathrm{L}} = \left(\frac{C_1 C_2}{C_1 + C_2} + C_{\mathrm{S}} \right) \tag{5.2}$$

C_{S} is the stray capacitance and can be minimized by short traces. Typical values range from 2 pF to 5 pF. The exact determination is important to let the device operate at its specified crystal frequency. For the power flower project, this means that this task is not *that* critical, since all the produced circuits are equal, so the stray component as the inner transistor capacitance of the micro-controller will be equal for all devices, and synchronization will not be affected.

For the used quartz crystal, the loading capacitance C_{L} is given by the data sheet with 6 pF to ∞, but there is also a hint in [59] to keep C_1 and C_2 as small as possible in order to avoid start-up problems. For the described circuit, a minimum C_1 and C_2 was calculated to be 12 pF.

Another Application note of [60] suggests a value C_1 and C_2 of 33 pF for exactly the same crystal.

The next topic is the drive level. It is given for the quartz with a maximum value of 1 µW. The resistor R_{S} in figure 5.1 is thought to regulate the current through the quartz crystal if it is too high. It is recommended to try the crystal with a bridged R_{S} because by choosing the right oscillating mode, it should work well. Measurements should be made. If the power at the crystal exceeds its maximum value, R_{S} has to be adopted. Typical values are between 40 kΩ to 100kΩ [59] [60].

5.3. Memory Organization

5.3.1. Program memory

The enhanced mid-range core has a program counter which is 15 bit wide and can address a 32k x 14 program memory space. The used *PIC®* controller has a program memory space of 2048 words, addressing memory regions above of 07FFh will cause a wrap-around in the memory space. The data of the program memory can be read either by the RETLW instruction or by pointing to the program memory setting a File Select Register [4] (FSR). Therefore, bit 7 of the FSRxH register is set and the corresponding INDx register is read.

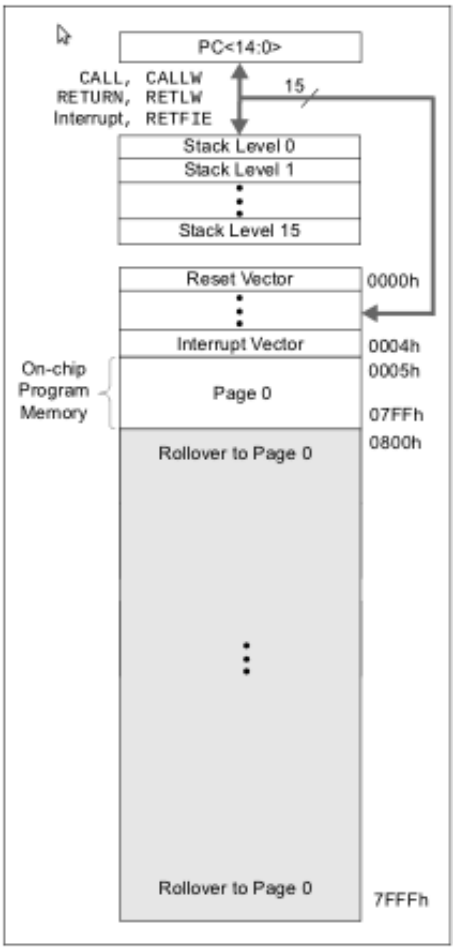

Figure 5.2.: Program Memory Organization of the *PIC® 16f639* [4]

5.3.2. Data memory

- 12 core registers which are the first 12 addresses of each data memory bank

  - INDF0
  - INDF1
  - PCL
  - STATUS: Arithmetic status of ALU, Reset Status
  - FSR0 Low
  - FSR0 High
  - FSR1 Low
  - FSR1 High
  - BSR
  - WREG
  - PCLATH
  - INTCON
- 20 Special Functions Register (SFR): used by the application to control peripheral functions in the device
- Up to 80 bytes of General Purpose Random Access Memory (GPR) in each data memory bank, can be accessed non-banked by FSR
- 16 bytes of common Random Access Memory (RAM) can be accessed from every bank
- Special Function Registers Summary
- Data Electrically Erasable Programmable Read-Only Memory (EEPROM)

5.3.3. Features for accessing and controlling program and data memory

- **PCL and PCLATH:** The lower byte of the 15-bit Program Counter (PC) of this micro-controller is delivered by the read- and writeable PCL register. Although, the second (high) byte of the counter is not directly read- or writeable, its value is determined by the PCLATH.
- **Stack:** The *PIC®16LF1823* has a 16-level x 15-bit wide hardware-implemented stack, which is not a part of program or data memory. It serves for saving the PC values in cases of CALL, CALLW or interrupt caused branches and can be POPed by other instructions.
- **Indirect Addressing:** INDFn are register representations which are not realized in the hardware. An instruction accessing one of them in reality accesses the register at the address defined in the FSR. 65536 locations can be addressed by the FSR. There are 3 regions of locations:
  - **Traditional Data Memory:** FSR 0x000 to FSR 0xFFF, those are the absolute addresses of SFR, GPR and common registers.

- **Linear Data Memory:** FSR 0x2000 to FSR 0x29AF, a virtually region that points to the 80-byte blocks of GPR. It is useful to implement buffers larger than 80 bytes. Common memory is not affected by the linear data memory region.
- **Program Flash Memory:** The program flash memory is mapped to the upper half of the FSR address space.

5.4. Output stage

As described in the previous chapters, the PFB should be able to generate sound by ringing a bell. To estimate the energy necessary for ringing a bell at an adequate level of sound volume, an experiment with the Christmas bell in figure 5.3 was performed.

To run the connected actor, a MOSFET in SOT23-6 housing like the *Zetex (Diodes Incorporated®) ZXGD3002E6* [61] is used in the PCB design. As an actor, a *Faulhaber 2230T003S* motor is used [62]. It has an energy-efficiency of almost 80% and needs a 3 V supply voltage. Support for calculating the electromechanic circumstances is given in [63].

Figure 5.3.: Christmas bell that helped estimating the required energy

By measuring the mass of the clapper, mounting it to a piece of twine, deflecting it to a certain height and releasing the clapper from this height, the energy stored in it in the

moment when it touches the bell can be calculated.

$$W_{\text{kin}} = W_{\text{pot}} = m \cdot g \cdot h \tag{5.3}$$

W_{kin}	Kinetic energy
W_{pot}	Potential energy
m	Mass
g	Acceleration of gravity

The real energy given to the bell is certainly less because of losses produced by the air resistance and friction.
So, $W_{\text{kin}} = W_{\text{pot}}$ represents an approximate level of energy which is given to the bell [64].

Actually, it is supposed that all the potential energy that is stored in the clapper released from the highest point, is converted to kinetic energy by accelerating. Since we neglect the losses, we consider that all the potential energy is given to the bell. Our *error* will be balanced by multiplying the result with a factor to also have some reserves left. Calculating these equations with the given values which are $m = 0{,}005\,\text{kg}$ $s = 5\,\text{cm}$ $g = 9{,}81\,\text{m/s}^2$ gives a result of W_{kin}=$\text{W}_{\text{pot}} = 0{,}002943\,\text{Ws}$.
Hence, the energy given to the bell is estimated to be 3 mWs. An efficiency of 30% is supposed. This means, 10 mWs of energy should be enough to trigger the bell at an acceptable sound level.

5.5. Serial Connection to a Personal Computer

For test and development activities, a serial interface (RS232) was implemented. The *PIC® 16LF1823*, described in chapter 5, comes up with an Enhanced Universal Synchronous Asynchronous Receiver Transmitter (EUSART) module, so it just has to be set up in the program code and can be used [4]. To convert the logic levels of the micro-controller to the RS232 standard, a MAX232 Chip is used. Therefore, a test program from [65] was downloaded. It was actually written for a *PIC® 18* device, but some small changes made it run on the *PIC® 16LF1823*. Since this is just an extended application of the device in a debug state which will not be needed in the final application there is no need to integrate the interface directly into the PCB board. Hence in the early prototyping phase, a small adapter wearing a *maxim integrated™ MAX 232 +5V-Powered, 2-channel RS-232 Driver/Receiver* [66] was constructed. It is powered from the test-board, so it is just this adapter that has to be connected to a personal computer running a serial terminal like *PuTTY* in *Microsoft® Windows* operating system or *GTKTerm*, which is supported by *ubuntu* operating system. Connecting four pins offers a real-time interface to a personal computer.

6. RF-module – Microchip MRF89XAM8A

The research process showed that the most economic and straight-forward option was to choose an RF transceiver module, which already comes with a radio-controller, antenna and peripheral parts. *Microchip®* offers the *MRF89XAM8A 868 MHz Ultra-Low Power Sub-GHz Transceiver Module*. It interacts via SPI with the *PIC®* Controller. The *MiWi* Protocol can be implemented with this hardware. This simple protocol is thought to be used where low data-rate, low distance and low cost are desired. Furthermore, the *MRF89XAM8A* supports data filtering/whitening/encoding.

Features:

- operating voltage range 2.1V-3.6V
- current consumption Receive (Rx) mode: 3 mA (typical)
- current consumption Transmit (Tx) mode: 25 mA at +10 dBm (typical)
- Sleep: 0,1 µA (typical)
- RF Output Power, Programmable with 8 Steps of typ. 3 dB
- super heterodyne architecture
- SPI

6.1. Interfacing to the Micro-Controller

Communication with the micro-controller is done through a 3-wire SPI connection, one chip select for data, one chip select for configuration, two interrupt request pins (IRQ0 and IRQ1) and a reset pin.

Data operation modes

- **continuous:** Each bit transmitted/received is directly accessible at the DATA pin. IRQ0 is not needed if sync and RSSI are not used. The PFB needs the RSSI. IRQ1 is not needed if Tx with Frequency Shift Keying (FSK) is not used (FSK 6dB less sensitivity but 12 times more data rate).
- **buffer:** Data is stored byte-wise in the First-In First-Out (FIFO) buffer, packet length is not limited. The FIFO can be emptied in stand-by mode. If none of the

relevant interrupt sources are needed, the interrupt pins IRQ0 and IRQ1 can be left open.

- **packet:** Packets are built automatically with preamble, sync word and encoding (optional). Maximum size of payload is 64 bytes. If none of the relevant interrupt sources are needed, the interrupt pins IRQ0 and IRQ1 can be left open.

6.2. Power consumption

At a data rate of 33,33 kbps, a 32-byte packet with a 4-byte preamble and a 4-byte start pattern takes about 10 ms to be transmitted [17]. In the transmit mode, with the maximum output power of +10 dB, the *MRF89XAM8A* consumes a maximum of 30 mA. Maximum current values result from using maximum voltage, which for this module is 3,6 V.
It is also assumed that, after sending, the device should be in receiving mode for 1 s. In this mode, the current consumption is rated with a maximum value of 3,5 mA at 3,6 V. This, all in all, provides an energy consumption for such a cycle of 1,8 mWs.

The real power consumption of this circuit part depends on the implemented communication method and on the strength needed for sending and the quantity of information. It will be investigated further during network development, as this was not possible for this project.

7. Electronic Implementation

7.1. Evaluation

The first evaluation steps of the micro-controller and the *bq25504 Ultra Low Power Boost Converter with Battery Management for Energy Harvester Applications* took place on a test breadboard as shown in figure 7.1. In the lower left corner, the *bq25504 Energy Harvesting carrier PCB board* was placed. Above, there is an electrolytic capacitor as a battery, the *PIC® 16LF1823*, a DC/DC converter for power supply and headers for programming and interfacing to a personal computer via RS232 (described in section 5.5).

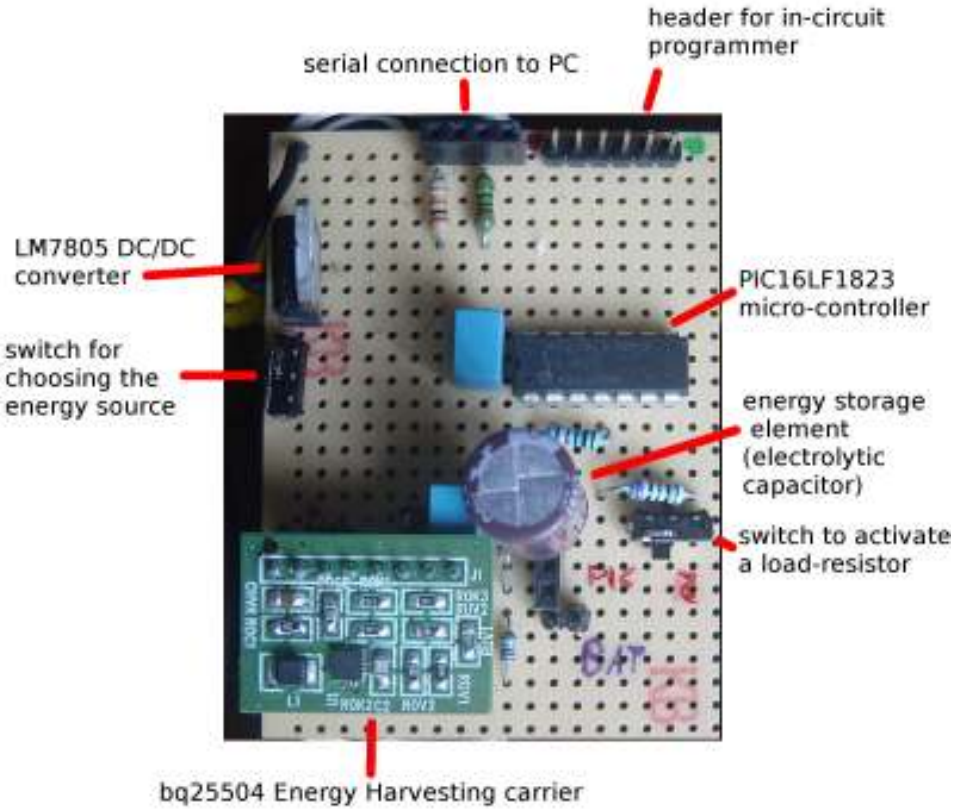

Figure 7.1.: Simple evaluation circuit

7.2. bq25504 Energy Harvesting carrier PCB board

The *bq25504* is just available in a 3 mm Quad-Flat-No Lead [5] (QFN) package. For evaluation, it has to be mounted on a PCB, or the evaluation board *bq25504 EVM* from *Texas Instruments Inc.* can be used. As there was the possibility to produce and solder PCB boards in the PCB prototype laboratory of the *Instituto Universitario de Microelectrónica Aplicada de la Universidad de Las Palmas de Gran Canaria*, this board was realized. Also several peripherals (C, Resistor (R), L) are mounted on this PCB, since it is recommended in the data sheet of the device to place them as closely to the pins of the chip as possible [53]. The schedule of the *bq25504 Energy Harvesting carrier PCB board* can be found in appendix C. The industry has debated the merits of both styles of land pads and although *Texas Instruments Inc.* recommends the copper defined style land pad (NSMD), both styles are acceptable for the use with the QFN/Small-Outline No Leads (SON) package [5].

7.3. PCB prototype

For final scheduling and routing of the whole circuit, the *KiCAD Electrical Design Automation (EDA) Suite* was used. This is an open-source software package for drawing schedules and laying out PCB circuits. The schedule was designed with *EEScheme*, and the board circuited was laid out with *PCBnew*. *PCBnew* supports the *freeROUTE* tool, which is a web-based *JAVA*™ plugin. To use it, a connection to the internet is required. *freeROUTE* extracts a *.dsn (Spectra Design File)* from *PCBnew*. This file is imported to *freeROUTE*, and by clicking on *Autoroute*, the whole PCB is laid out automatically, based on the design rules defined in *PCBnew* before exporting the *.dsn* file. For a positive result, it is necessary to place the parts in *PCBnew* in a way that permits enough space for routes, otherwise *freeROUTE* will not terminate but stay in an endless loop trying to resolve routing tasks. After routing, the layout is automatically optimized in order to achieve short circuit paths and a small number of vias. The PCB of the Power Flower Bell (PFB) was laid out by *freeROUTE* and optimized later in *PCBnew* manually.
In general, *freeROUTE* seems to be a quite efficient tool for auto-routing. Compared to commercial systems, the *KiCAD EDA Suite* is an open-source alternative for small- to mid-size projects. The possibilities of realizing complex details in multi-layer circuits are not implemented deeply. Also, simulation has to be done externally. Once used for the commands, it permits fast and intuitive editing. It is possible to directly generate a 3D view of the board with soldered parts in *PCBnew*. Figure 7.2 is a 3D view of the developed PCB board.

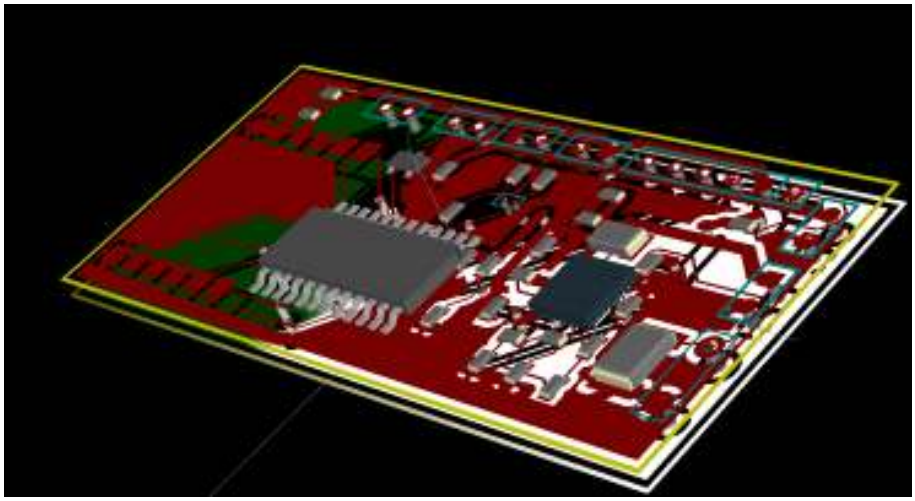

Figure 7.2.: 3D View of the PCB by *PCBnew*

For the PCB design, the Zetex MOSFET in a SOC23 housing was supposed [67]. The values of R_{OC1}, R_{OC2} serve for programming the maximum power point tracking (see also chapter 4.1.2). They have to be set up with the data obtained by testing the earth battery.

8. Conclusion

The work on the presented project showed that, in principle, it is possible to run low-power electronic devices like sensors or actors by a dirt-battery. A Power Flower Bell (PFB) device can be seen as such a device. Even if the amount of extracted energy is quite low, it can be a model for other applications. The dirt-battery, in its current state, can be developed further by optimizing the composition of the soil and the used diaphragm. Moreover, there might be applications, where galvanic energy is available as an unused source.

This work is one of a few available publications describing dirt-batteries. Much of the information about this topic found on the internet is not scientific but sometimes even esoteric. All other systems found are driven by a serial set up of dirt batteries. The here presented system is based on *one* single cell of a dirt-battery, which is much easier to install.

The designed circuit can also be powered by many other kinds of DC low-power sources. There are certainly new possibilities for artists who want to realize a wireless networking, energy harvesting driven sound installation.

The integration of the RF part into the PFB circuit was not done during the project. However, the basics of this part of the system are described in the present document.

Even if the dirt-battery is not yet optimized, its functionality could be shown. In deed, it was possible to ring a bell with the energy stored in the used supercap by the PFB. A low-price vibrating motor usually used in cell phones was used.

Bibliography

[1] T. Kazmierski and S. Beeby, *Energy Harvesting Systems*. England: Springer, 2010, ISBN: 978-1441975652.

[2] M. C. électroacoustique canadienne Canadian Electroacoustic Community, "econtact 11.3 – logiciels audio open source open source for audio application," 11.02.2013. [Online]. Available: http://cec.sonus.ca/econtact/11_3/AAAAritsch_zmoelnig_iem.html

[3] J. Ebert, "Wireless communication networks and protocols," LV, 2012.

[4] Microchip®, *PIC® 12F/LF1822/PIC16F/LF1823 Data sheet*, 2010.

[5] S. Kummerl, B. Lange, and D. Nguyen, "QFN/**SON!** (**SON!**) PCB attachment," *Application Report - Texas instruments*, vol. SLUA271A, 2002.

[6] W. Ritsch, "Power flower bell network - idea of an electric sound installation," internal use only, 11 2011.

[7] M. staps, "Soil lamp," 09.05.2012. [Online]. Available: http://www.mariekestaps.nl/?/Design/Soil-Lamp-2/

[8] P. Harrop, "The glamorous world of energy harvesting," 01.04.2012. [Online]. Available: http://www.energyharvestingjournal.com/articles/the-glamorous-world-of-energy-harvesting-00002083.asp?sessionid=1

[9] E. E. González, "Diseño de un sistema de captacion de energia residual basado en el acondicionador EH300 de la empresa ADVANCED LINEAR DEVICES," Master's thesis, ULPGC, March 2010.

[10] Mstaps, "Soil clock," 16.12.2012. [Online]. Available: http://www.mariekestaps.nl/new/?/Design/Soil-Clock-1/

[11] R. Chao, "Making low-voltage energy harvesting practical: Part 3the future of micro-power energy harvesting," 2012.08.08. [Online]. Available: http://www2.electronicproducts.com/Making_low_voltage_energy_harvesting_practical_Part_3The_future_of_micro_power_energy_harvesting-article-fapo_ALD_aug2012-html.aspx

[12] T. E. Bonnerud, "Rosige zukunft für ultra-low-power-funktechnik," *Wireless Telegraph*, 2011.

[13] Bundesnetzagentur, "ISM-Definition," 09.01.2012. [Online]. Available: http://www.bundesnetzagentur.de/cln_1932/DE/Sachgebiete/Telekommunikation/RegulierungTelekommunikation/Frequenzordnung/Allgemeinzuteilungen/ISMFrequenzen_Basepage.html

[14] ITWissen, "ISM (industrial, scientific, and medical)," 09.05.2012. [Online]. Available: http://www.itwissen.info/definition/lexikon/ISM-Band-ISM-industrial-scientific-and-medical.html

[15] M. Gerstner, "Zigbee," Master's thesis, TU Wien, 2010.

[16] Microchip®, *Microchip® MRF89XAM8A data sheet*, Microchip® Technology Inc., 2010.

[17] Microchip®, *MRF89XA datasheet*, 2010-2011.

[18] Telecom ABC, "Isotropic antenna," 13.01.2013. [Online]. Available: http://www.telecomabc.com/i/isotropic.html

[19] ITWissen, "IEEE 802.15.4," 14.06.2012. [Online]. Available: http://www.itwissen.info/definition/lexikon/802-15-4-IEEE-802-15-4.html

[20] Wikipedia, "Amplitudenmodulation mit unterdrücktem Träger," 09.05.2012. [Online]. Available: http://de.wikipedia.org/wiki/Amplitudenmodulation_mit_unterdr%C3%BCcktem_Tr%C3%A4ger

[21] Texas Instruments, *CC2570 CC2571 1- and 8-Channel ANT TM RF Network Processors*, March 2011.

[22] ITWissen, "Ad-hoc network," 2012.05.15. [Online]. Available: http://www.itwissen.info/definition/lexikon/Ad-hoc-Netzwerk-ad-hoc-network.html

[23] thisisant.com, "ANT message protocol and usage." [Online]. Available: http://www.thisisant.com/pages/developer-zone/ant-protocol-and-usage

[24] W. Ongena, "Was ist DECT ULE," *Markt und Technik*, vol. 45, p. 17, 2011.

[25] W. Ritsch, "Vision and context of the power flower bells network," 13.1.2012. [Online]. Available: http://algo.mur.at/projects/powerflowerbells/vision

[26] Labor für Prozessdatenverarbeitung der Hochschule Reutlingen, "Übersicht nutzbarer Energiequellen für Energy Harvesting," 02.04.2012. [Online]. Available: http://www.harvesting-energy.de/

[27] I. Lehnen-Beyel, "Bakterien machen aus Zucker elektrischen Strom," 03.04.2012. [Online]. Available: http://www.wissenschaft.de/wissenschaft/news/228138

[28] orf.at, "Ölfressende Bakterien erzeugen Strom," 03.04.2012. [Online]. Available: http://sciencev1.orf.at/science/news/39927

[29] S. Boisseau and G. Despesse, "Energy harvesting, wireless sensor networks & opportunities for industrial applications," 2012.08.08. [Online]. Available: http://www.eetimes.com/design/smart-energy-design/4237022/Energy-harvesting--wireless-sensor-networks---opportunities-for-industrial-applications?pageNumber=2

[30] www.economicexpert.com, "Earth battery," 2012.04.02. [Online]. Available: http://www.economicexpert.com/a/Earth:battery.htm

[31] J. Layton, "How soil lamps work," 31.03.2012. [Online]. Available: http://science.howstuffworks.com/environmental/green-tech/sustainable/soil-lamp.htm

[32] Hila Research Center at Hila Science Camp, Turnbull School, "Lemon battery," 14.01.2013. [Online]. Available: http://www.hilaroad.com/camp/projects/lemon/lemon_battery.html

[33] Wikipedia, "Daniell element," 11.12.2012. [Online]. Available: http://de.wikipedia.org/w/index.php?title=Datei:NMAH-Daniell_cell_batteries_1836.JPG&filetimestamp=20110515192338

[34] Institut für Physikalische und Theoretische Chemie der Technischen Universität Carolo-Wilhelmina zu Braunschweig, "Elektrodenreaktionen und galvanische Zellen," 06.12.2012. [Online]. Available: http://www.pci.tu-bs.de/aggericke/PC1/Kap_VI/Elektrodenreak_Galvanische_Ketten.htm

[35] Wikipedia, "Galvanic cell," 20.02.2013. [Online]. Available: http://en.wikipedia.org/wiki/Galvanic_cell

[36] C. G. Hönck, "Kupfer satt," 14.01.2013. [Online]. Available: http://www.greenpeace-magazin.de/index.php?id=5347

[37] Pancontrol, *70A Datenblatt*.

[38] R. A. Cullen, "What is maximum power point tracking (mppt) and how does it work?"

[39] M. Dirjish, "What is the difference between thin-film and crystalline-silicon solar panels," 06.01.2013. [Online]. Available: http://electronicdesign.com/power-sources/what-s-difference-between-thin-film-and-crystalline-silicon-solar-panels

[40] Solarserver, "Photovoltaik: Solarstrom und Solarzellen in Theorie und Praxis," 13.08.2012. [Online]. Available: http://www.solarserver.de/wissen/basiswissen/photovoltaik.html

[41] National Instruments™, "Photovoltaic cell overview," 13.08.2012. [Online]. Available: http://www.ni.com/white-paper/7229/en

[42] C.-C. Wu, "Overview of solar cell technologies," 13.08.2012. [Online]. Available: http://www.google.at/url?sa=t&rct=j&q=&esrc=s&source=web&cd=2&ved=0CFQQFjAB&url=http%3A%2F%2Fforesight.iis.sinica.edu.tw%2Fproposal%2F2008%2FPDF%2FOverview%2520of%2520Solar%2520Cell%2520Technologies.pdf&ei=WaIoUMq0E4vmtQaPv4HABg&usg=AFQjCNE2UXYZqJO823fKjGiUUxDaW-w5LQ

[43] sunnyBAG®, "Sunnybag story," 16.12.2012. [Online]. Available: http://www.sunnybag.at/pages/geschichte

[44] http://www.mpoweruk.com, "Graetzel cells," 06.02.2013. [Online]. Available: http://www.mpoweruk.com/gratzel.htm

[45] Tikalon LLC, "Dye-sensitized solar cells," 06.02.2013. [Online]. Available: http://tikalon.com/blog/blog.php?article=graetzel&sidebar=050610

[46] R. Kartusch, "Die Graetzel Zelle," 06.02.2013. [Online]. Available: http://www.univie.ac.at/pph/ecophys/photobio/doc/GraetzelZelle.pdf

[47] http://www.mpoweruk.com, "Thermocouple electric generators," 06.02.2013. [Online]. Available: http://www.mpoweruk.com/thermoelectricity.htm

[48] BioLite™, "biolitestove," 16.12.2012. [Online]. Available: http://www.biolitestove.com/homestove/home-stories/view-all-home/

[49] micropelt, *TE-CORE6/TE-CORE7 Thermo Harvesting Powser Module*, 2012.

[50] Y. K. Ramadass and A. P. Chandrakasan, "An efficient piezoelectric energy harvesting interface circuit using a bias-flip rectifier and shared inductor," *MIT Open Acces Articles*, 2010.

[51] Linear Technology Corporation, *LTC3188-1 Piezoelectric Energy Harvesting Power Supply datasheet*.

[52] hearst Electronic Magazine, "Texas Instruments: Boosting extremely low power makes energy harvesting very attractive," 2012.08.08. [Online]. Available: http://www2.electronicproducts.com/Boosting_extremely_low_power_makes_energy_harvesting_very_attractive-article-poypo_TI_bq25504_jan2012-html.aspx

[53] Texas Instruments, *bq25504 datasheet*, 2011.

[54] J. Rehrmann, "Das neue InterNetzteil- und Konverter-Handbuch von Dipl.-Ing Jörg Rehrmann," 25.08.2012. [Online]. Available: http://www.joretronik.de/Web_NT_Buch/Kap6_2/Kapitel6_2.html

[55] COILGUN SYSTEMS, "Voltage converter design 1," 11.02.2013. [Online]. Available: http://www.coilgun.eclipse.co.uk/electromagnetic_pistol_voltage_converter_design.html

[56] Institut für Elektronik, TU Graz, "Elektronische Schaltungstechnik 3," Class, 2003/2004.

[57] B. Ivey, *Low Power Design Guide*, Microchip Technology Inc., 2011.

[58] Microchip Technology Inc., *PIC12F635/PIC16F636/639 data sheet*, 2007.

[59] S. Bible, *AN826 Crystal Oscillator Basics and Crystal Selection for rfPICTM and PICmicro® devices*, Microchip Technology Inc., 2002.

[60] D. Matthews, *AN849 Basic PICmicro Oscillator Design*, Microchip Technology, Inc., 2002.

[61] ZETEX Semiconductors, *Zetex E3002E6 datasheet*, October 2007.

[62] DR. FRITZ FAULHABER GMBH & CO. KG, *Faulhaber 2230 datasheet*.

[63] ——, *Technische Informationen*, 2012-2013.

[64] R. Fitzpatrick, "Energy conservation during free-fall," 2012.04.04. [Online]. Available: http://farside.ph.utexas.edu/teaching/301/lectures/node57.html

[65] MicrochipC.com, "C sample code for pic micros and hi-tech c," 2012.06.13. [Online]. Available: http://www.microchipc.com/sourcecode/

[66] maxim integrated, *+5V-Powered, Multichannel RS-232 Drivers/Receivers datasheet*, 2010.

[67] ZETEX Semiconductors, *30V N-CHANNEL ENHANCEMENT MODE MOSFET datasheet*, October 2005.

[68] J. Barton, "Electrochemical series," 04.02.2013. [Online]. Available: http://www.swapyournotes.com/articledetail.html/438

9. Appendix

Appendix A.

Electrochemical series

$F_2(g) + 2e^-$	$\rightarrow$	$2F^-(aq)$	+2.87
$Au^+(aq) + e^-$	$\rightarrow$	$Au(s)$	+1.68
$Cl_2(g) + 2e^-$	$\rightarrow$	$2Cl^-(aq)$	+1.36
$O_2(g) + 4H^+(aq) + 4e^-$	$\rightarrow$	$2H_2O(1)$	+1.23
$Ag^+(aq) + e^-$	$\rightarrow$	$Ag(s)$	+0.80
$Fe^{3+}(aq) + e^-$	$\rightarrow$	$Fe^{2+}(aq)$	+0.77
$I_2(s) + 2e^-$	$\rightarrow$	$2I^-(aq)$	+0.54
$O_2(g) + 2H_2O(l) + 4e^-$	$\rightarrow$	$4OH^-(aq)$	+0.40
$Cu^{2+}(aq) + 2e^-$	$\rightarrow$	$Cu(s)$	+0.34
$2H^+(aq) + 2e^-$	$\rightarrow$	$H_2(g)$	0.00
$Pb^{2+}(aq) + 2e^-$	$\rightarrow$	$Pb(s)$	−0.13
$Sn^{2+}(aq) + 2e^-$	$\rightarrow$	$Sn(s)$	−0.14
$Ni^{2+}(aq) + 2e^-$	$\rightarrow$	$Ni(s)$	−0.23
$Co^{2+}(aq) + 2e^-$	$\rightarrow$	$Co(s)$	−0.28
$Fe^{2+}(aq) + 2e^-$	$\rightarrow$	$Fe(s)$	−0.44
$Zn^{2+}(aq) + 2e^-$	$\rightarrow$	$Zn(s)$	−0.76
$2H_2O(l) + 2e^-$	$\rightarrow$	$H_2(g) + 2OH^-(aq)$	−0.83
$Al^{3+}(aq) + 3e^-$	$\rightarrow$	$Al(s)$	−1.67
$Mg^{2+}(aq) + 2e^-$	$\rightarrow$	$Mg(s)$	−2.34
$Na^+(aq) + e^-$	$\rightarrow$	$Na(s)$	−2.71
$Ca^{2+}(aq) + 2e^-$	$\rightarrow$	$Ca(s)$	−2.87
$K^+(aq) + e^-$	$\rightarrow$	$K(s)$	−2.93

Figure A.1.: The electrochemical series [68]
The values in the right column indicate the standard potentials in Volts.

Appendix B.

Dirt-battery output power measurements

B.1. Cubic dirt-battery without diaphragm, without copper-nitrate

Table B.1.: Dirt-battery

$R[\Omega]$	U [V]	I [A]	P[W]
1	0.003	0.0030	0.0090
2	0.006	0.0030	0.0180
3	0.008	0.0027	0.0213
4	0.011	0.0027	0.0302
5	0.013	0.0026	0.0338
6	0.016	0.0027	0.0427
7	0.018	0.0026	0.0463
8	0.021	0.0026	0.0551
9	0.023	0.0026	0.0588
10	0.028	0.0028	0.0784
20	0.049	0.0024	0.1201
30	0.070	0.0023	0.1633
40	0.092	0.0023	0.2116
50	0.111	0.0022	0.2464
60	0.126	0.0021	0.2646
70	0.143	0.0020	0.2921
80	0.160	0.0020	0.3200
90	0.175	0.0019	0.3403
100	0.190	0.0019	0.3610
200	0.295	0.0015	0.4351
300	0.371	0.0012	0.4588
400	0.424	0.0011	0.4494

Batt. Nr:	X	Test	I
500	0.467	0.0009	0.4362
600	0.502	0.0008	0.4200
700	0.530	0.0008	0.4013
800	0.556	0.0007	0.3864
900	0.580	0.0006	0.3738
1k	0.602	0.0006	0.3624
2k	0.708	0.0004	0.2506
3k	0.750	0.0003	0.1875
4k	0.774	0.0002	0.1498
5k	0.790	0.0002	0.1248
6k	0.802	0.0001	0.1072
7k	0.810	0.0001	0.0937
8k	0.816	0.0001	0.0832
9k	0.823	0.0001	0.0753
10k	0.829	0.0001	0.0687
20k	0.845	0.0000	0.0357
30k	0.851	0.0000	0.0241
40k	0.854	0.0000	0.0182
50k	0.856	0.0000	0.0147
60k	0.857	0	0.0122
70k	0.858	0	0.0105
80k	0.858	0	0.0092
90k	0.860	0	0.0082
100k	0.8690	0	0.0076

B.2. Two cylindrical dirt-batteries in variations

For the meaning of the indices please refer to 3.1.5.

Table B.2.: Dirt-Battery Comparison

$R[\Omega]$	U_{BNNC} [V]	U_{BNNL} [V]	U_{BDNC} [V]	U_{SNN} [V]	U_{SDN} [V]	U_{SNC} [V]	U_{BDCC} [V]	U_{BNCC} [V]	U_{SDC} [V]
1	0,008	0,008	0,003	0,003	0,001	0,005	0,005	0,008	0,003
2	0,016	0,015	0,006	0,005	0,002	0,008	0,009	0,015	0,005
3	0,022	0,022	0,009	0,007	0,002	0,013	0,014	0,023	0,009
4	0,029	0,028	0,013	0,010	0,003	0,016	0,018	0,030	0,012
5	0,036	0,035	0,016	0,012	0,004	0,020	0,022	0,037	0,014

Batt. Nr:	X	Test	I						
6	0,043	0,041	0,019	0,015	0,005	0,024	0,026	0,043	0,017
7	0,049	0,048	0,022	0,017	0,006	0,028	0,030	0,050	0,020
8	0,055	0,054	0,025	0,019	0,007	0,032	0,034	0,056	0,022
9	0,061	0,060	0,028	0,022	0,007	0,035	0,038	0,062	0,025
10	0,072	0,072	0,033	0,026	0,009	0,041	0,045	0,072	0,029
20	0,123	0,122	0,059	0,046	0,017	0,074	0,080	0,124	0,053
30	0,168	0,161	0,084	0,066	0,025	0,105	0,112	0,171	0,076
40	0,213	0,204	0,111	0,088	0,035	0,137	0,146	0,215	0,101
50	0,249	0,239	0,133	0,106	0,042	0,164	0,174	0,251	0,122
60	0,277	0,266	0,152	0,122	0,049	0,186	0,197	0,277	0,140
70	0,304	0,295	0,172	0,138	0,056	0,208	0,220	0,305	0,158
80	0,332	0,328	0,192	0,155	0,065	0,231	0,245	0,335	0,177
90	0,355	0,342	0,208	0,170	0,072	0,251	0,265	0,358	0,194
100	0,377	0,364	0,231	0,184	0,079	0,268	0,284	0,380	0,209
200	0,506	0,502	0,351	0,290	0,141	0,403	0,416	0,515	0,331
300	0,579	0,572	0,432	0,368	0,193	0,488	0,500	0,588	0,415
400	0,624	0,615	0,487	0,424	0,237	0,545	0,555	0,634	0,477
500	0,655	0,646	0,527	0,468	0,275	0,588	0,594	0,666	0,523
600	0,677	0,668	0,558	0,506	0,308	0,619	0,623	0,690	0,558
700	0,695	0,687	0,583	0,535	0,337	0,645	0,645	0,706	0,587
800	0,709	0,702	0,603	0,563	0,364	0,667	0,666	0,721	0,612
900	0,723	0,716	0,619	0,583	0,387	0,684	0,682	0,733	0,631
1000	0,732	0,722	0,642	0,606	0,408	0,698	0,694	0,746	0,644
2000	0,775	0,771	0,716	0,706	0,542	0,778	0,759	0,784	0,737
3000	0,791	0,788	0,743	0,746	0,611	0,812	0,782	0,801	0,775
4000	0,797	0,797	0,759	0,770	0,654	0,832	0,794	0,809	0,796
5000	0,802	0,803	0,768	0,784	0,684	0,845	0,802	0,814	0,810
6000	0,805	0,806	0,774	0,795	0,705	0,855	0,807	0,816	0,819
7000	0,807	0,810	0,779	0,804	0,721	0,862	0,811	0,819	0,826
8000	0,808	0,813	0,783	0,810	0,735	0,868	0,814	0,821	0,831
9000	0,809	0,814	0,786	0,815	0,744	0,873	0,816	0,822	0,836
10000	0,815	0,815	0,788	0,819	0,753	0,877	0,819	0,824	0,839
OC	0,824	0,824	0,808	0,853	0,844	0,923	0,836	0,831	0,875

B.3. Octave/MATLAB® scripts

B.3.1. Earthbattery - theoretical consideration

This script was just used to show the envelope of the function y expressed in equation 3.13.

```
x=[0:0.1:5];
y=x./((x.^2)+1)
figure;
plot(x,y,'LineWidth',2)
xlabel('x');
ylabel('y');
print("earth_theory.png","-color","-dpng")
```

B.3.2. Comparison of two cylindric dirt-batteries

The following code was used to obtain figure 3.12 and figure 3.11. It is based on the data in table B.2.

```
%Soil Leitnergasse complete Test 1ohm to 100kohm
%detail up to 1okohm, higher values of resistors
%can not lead to higher output powers
R_whole_10=[1,2,3,4,5,6,7,8,9,10,20,30,40,50,60,70,80,90,100,
200,300,400,500,600,700,800,900,1000,2000,3000,4000,5000,6000,
7000,8000,9000,10000];
Length_whole_10 = length(R_whole_10);


%(B)...big
%(S)...Small
%(N)...No
%(D)...Diaphragma
%(C)...Copper
%(L)...Limit
%(C) ...Centered

%U big (B), no diaphragma (N), no copper nitrate (N), zinc centered (C)
%-------------------------------------------------------------------------
U_whole_10_BNNC = [0.008, 0.016, 0.022, 0.029, 0.036, 0.043, 0.049, 0.055, 0.061, 0.072, 0.123,
     0.168, 0.213, 0.249, 0.277, 0.304, 0.332, 0.355, 0.377, 0.506, 0.579, 0.624, 0.655, 0.677, 0.695,
      0.709, 0.723, 0.732, 0.775, 0.791, 0.797, 0.802, 0.805, 0.807, 0.808, 0.809, 0.815];
U_whole_10_BNNC_OC = 0.824;
I_whole_10_BNNC=U_whole_10_BNNC./R_whole_10;
P_whole_10_BNNC=U_whole_10_BNNC.*I_whole_10_BNNC;
%Calculate Power to mW
P_whole_10_BNNC_mW=P_whole_10_BNNC.*1000;
%find absolute voltage at MPP
P_max_BNNC = max(P_whole_10_BNNC);
[Y,I] = max(P_whole_10_BNNC);
U_maxp_BNNC = U_whole_10_BNNC(I);
MPP_BNNC = U_maxp_BNNC/U_whole_10_BNNC_OC;

%U big (B), no diaphragma (N), no copper nitrate (N), zinc at limit (L)
%-------------------------------------------------------------------------
U_whole_10_BNNL = [0.008, 0.015, 0.022, 0.028, 0.035, 0.041, 0.048, 0.054, 0.060, 0.072, 0.122,
     0.161, 0.204, 0.239, 0.266, 0.295, 0.328, 0.342, 0.364, 0.502, 0.572, 0.615, 0.646, 0.668, 0.687,
      0.702, 0.716, 0.722, 0.771, 0.788, 0.797, 0.803, 0.806, 0.810, 0.813, 0.814, 0.815];
U_whole_10_BNNL_OC = 0.824;
I_whole_10_BNNL=U_whole_10_BNNL./R_whole_10;
P_whole_10_BNNL=U_whole_10_BNNL.*I_whole_10_BNNL;
P_whole_10_BNNL_mW=P_whole_10_BNNL.*1000;
P_max_BNNL = max(P_whole_10_BNNL);
[Y,I] = max(P_whole_10_BNNL);
U_maxp_BNNL = U_whole_10_BNNL(I);
MPP_BNNL = U_maxp_BNNL/U_whole_10_BNNL_OC;

%U big (B), with diaphragma (D), no copper nitrate (N), zinc centered (C)
%-------------------------------------------------------------------------
U_whole_10_BDNC = [0.003, 0.006, 0.009, 0.013, 0.016, 0.019, 0.022, 0.025, 0.028, 0.033, 0.059,
     0.084, 0.111, 0.133, 0.152, 0.172, 0.192, 0.208, 0.231, 0.351, 0.432, 0.487, 0.527, 0.558, 0.583,
      0.603, 0.619, 0.642, 0.716, 0.743, 0.759, 0.768, 0.774, 0.779, 0.783, 0.786, 0.788];
U_whole_10_BDNC_OC = 0.808;
I_whole_10_BDNC=U_whole_10_BDNC./R_whole_10;
P_whole_10_BDNC=U_whole_10_BDNC.*I_whole_10_BDNC;
P_whole_10_BDNC_mW=P_whole_10_BDNC.*1000;
P_max_BDNC = max(P_whole_10_BDNC);
```

```
[Y,I] = max(P_whole_10_BDNC);
U_maxp_BDNC = U_whole_10_BDNC(I);
MPP_BDNC = U_maxp_BDNC/U_whole_10_BDNC_OC;

%U small (S), no diaphragma (N), no copper nitrate (N)
%-------------------------------------------------------
U_whole_10_SNN = [0.003, 0.005, 0.007, 0.010, 0.012, 0.015, 0.017, 0.019, 0.022, 0.026, 0.046, 0.066,
      0.088, 0.106, 0.122, 0.138, 0.155, 0.170, 0.184, 0.290, 0.368, 0.424, 0.468, 0.506, 0.535,
     0.563, 0.583, 0.606, 0.706, 0.746, 0.770, 0.784, 0.795, 0.804, 0.810, 0.815, 0.819];
U_whole_10_SNN_OC = 0.853;
I_whole_10_SNN=U_whole_10_SNN./R_whole_10;
P_whole_10_SNN=U_whole_10_SNN.*I_whole_10_SNN;
P_whole_10_SNN_mW=P_whole_10_SNN.*1000;
P_max_SNN = max(P_whole_10_SNN);
[Y,I] = max(P_whole_10_SNN);
U_maxp_SNN = U_whole_10_SNN(I);
MPP_SNN = U_maxp_SNN/U_whole_10_SNN_OC;

%U small (S), with diaphragma (D), no copper nitrate (N)
%-------------------------------------------------------
U_whole_10_SDN = [0.001, 0.002, 0.002, 0.003, 0.004, 0.005, 0.006, 0.007, 0.007, 0.009, 0.017, 0.025,
      0.035, 0.042, 0.049, 0.056, 0.065, 0.072, 0.079, 0.141, 0.193, 0.237, 0.275, 0.308, 0.337,
     0.364, 0.387, 0.408, 0.542, 0.611, 0.654, 0.684, 0.705, 0.721, 0.735, 0.744, 0.753]
U_whole_10_SDN_OC = 0.844;
I_whole_10_SDN=U_whole_10_SDN./R_whole_10;
P_whole_10_SDN=U_whole_10_SDN.*I_whole_10_SDN;
P_whole_10_SDN_mW=P_whole_10_SDN.*1000;
P_max_SDN = max(P_whole_10_SDN);
[Y,I] = max(P_whole_10_SDN);
U_maxp_SDN = U_whole_10_SDN(I);
MPP_SDN = U_maxp_SDN/U_whole_10_SDN_OC;

%U small (S), no diaphragma (N), with copper nitrate (C)
%-------------------------------------------------------
U_whole_10_SNC = [0.005, 0.008, 0.013, 0.016, 0.020, 0.024, 0.028, 0.032, 0.035, 0.041, 0.074, 0.105,
      0.137, 0.164, 0.186, 0.208, 0.231, 0.251, 0.268, 0.403, 0.488, 0.545, 0.588, 0.619, 0.645,
     0.667, 0.684, 0.698, 0.778, 0.812, 0.832, 0.845, 0.855, 0.862, 0.868, 0.873, 0.877]
U_whole_10_SNC_OC = 0.923;
I_whole_10_SNC=U_whole_10_SNC./R_whole_10;
P_whole_10_SNC=U_whole_10_SNC.*I_whole_10_SNC;
P_whole_10_SNC_mW=P_whole_10_SNC.*1000;
P_max_SNC = max(P_whole_10_SNC);
[Y,I] = max(P_whole_10_SNC);
U_maxp_SNC = U_whole_10_SNC(I)
MPP_SNC = U_maxp_SNC/U_whole_10_SNC_OC;

%U big (B), with diaphragma (D), with copper nitrate (C), zinc centered (C)
%-------------------------------------------------------------------------
U_whole_10_BDCC = [0.005, 0.009, 0.014, 0.018, 0.022, 0.026, 0.030, 0.034, 0.038, 0.045, 0.080,
      0.112, 0.146, 0.174, 0.197, 0.220, 0.245, 0.265, 0.284, 0.416, 0.500, 0.555, 0.594, 0.623, 0.645,
      0.666, 0.682, 0.694, 0.759, 0.782, 0.794, 0.802, 0.807, 0.811, 0.814, 0.816, 0.819]
U_whole_10_BDCC_OC = 0.836;
I_whole_10_BDCC=U_whole_10_BDCC./R_whole_10;
P_whole_10_BDCC=U_whole_10_BDCC.*I_whole_10_BDCC;
P_whole_10_BDCC_mW=P_whole_10_BDCC.*1000;
P_max_BDCC = max(P_whole_10_BDCC);
[Y,I] = max(P_whole_10_BDCC);
U_maxp_BDCC = U_whole_10_BDCC(I);
MPP_BDCC = U_maxp_BDCC/U_whole_10_BDCC_OC;

%U big (B), no diaphragma (N), with copper nitrate (C), zinc centered (C)
%-------------------------------------------------------------------------
U_whole_10_BNCC = [0.008, 0.015, 0.023, 0.030, 0.037, 0.043, 0.050, 0.056, 0.062, 0.072, 0.124,
      0.171, 0.215, 0.251, 0.277, 0.305, 0.335, 0.358, 0.380, 0.515, 0.588, 0.634, 0.666, 0.690, 0.706,
      0.721, 0.733, 0.746, 0.784, 0.801, 0.809, 0.814, 0.816, 0.819, 0.821, 0.822, 0.824]
U_whole_10_BNCC_OC = 0.831;
I_whole_10_BNCC=U_whole_10_BNCC./R_whole_10;
P_whole_10_BNCC=U_whole_10_BNCC.*I_whole_10_BNCC;
P_whole_10_BNCC_mW=P_whole_10_BNCC.*1000;
P_max_BNCC = max(P_whole_10_BNCC);
[Y,I] = max(P_whole_10_BNCC);
U_maxp_BNCC = U_whole_10_BNCC(I);
MPP_BNCC = U_maxp_BNCC/U_whole_10_BNCC_OC;

%U small (S), with diaphragma (D), with copper nitrate (C)
%---------------------------------------------------------
U_whole_10_SDC = [0.003, 0.005, 0.009, 0.012, 0.014, 0.017, 0.020, 0.022, 0.025, 0.029, 0.053, 0.076,
      0.101, 0.122, 0.140, 0.158, 0.177, 0.194, 0.209, 0.331, 0.415, 0.477, 0.523, 0.558, 0.587,
     0.612, 0.631, 0.644, 0.737, 0.775, 0.796, 0.810, 0.819, 0.826, 0.831, 0.836, 0.839]
U_whole_10_SDC_OC = 0.875;
I_whole_10_SDC=U_whole_10_SDC./R_whole_10;
P_whole_10_SDC=U_whole_10_SDC.*I_whole_10_SDC;
P_whole_10_SDC_mW=P_whole_10_SDC.*1000;
P_max_SDC = max(P_whole_10_SDC);
[Y,I] = max(P_whole_10_SDC);
U_maxp_SDC = U_whole_10_SDC(I);
MPP_SDC = U_maxp_SDC/U_whole_10_SDC_OC;


%build MPP vector of relations V_MPP/V_opencircuit
```

```
MPP = [MPP_BNNC, MPP_BNNL, MPP_BNCC, MPP_SNN, MPP_SNC, MPP_BDCC, MPP_BDNC, MPP_SDN,  MPP_SDC]


%Plot absolute power curves
figure;
hold on
plot(R_whole_10,P_whole_10_BNNC_mW,'g','LineWidth',2)
plot(R_whole_10,P_whole_10_BNNL_mW,'r','LineWidth',2)
plot(R_whole_10,P_whole_10_BNCC_mW,'*','LineWidth',1)
plot(R_whole_10,P_whole_10_BDCC_mW,'k','LineWidth',2)
plot(R_whole_10,P_whole_10_BDNC_mW,'b','LineWidth',2)
plot(R_whole_10,P_whole_10_SNN_mW,'y','LineWidth',2)
plot(R_whole_10,P_whole_10_SDN_mW,'m','LineWidth',2)
plot(R_whole_10,P_whole_10_SNC_mW,'c','LineWidth',2)
plot(R_whole_10,P_whole_10_SDC_mW,'o','LineWidth',1)
hold off
legend('BNNC','BNNL','BNCC','BDCC','BDNC','SNN','SDN','SNC','SDC')
%title('Comparison of ou');
xlabel('R [Ohm] ');
ylabel('P - e - a - r - t - h [mW] ');
print("absolute_power.png","-color","-dpng")

%Plot Spannungsverhltnisse maxp/ll

figure;
bar (MPP)
ylabel('MPP relation');
xlabel('Types of Dirtbatteries')
set (gca, 'xtick', [1 2 3 4 5 6 7 8 9])
set(gca, 'xticklabel',{'BNNC', 'BNNL', 'BNCC', 'SNN', 'SNC', 'BDCC', 'BDNC', 'SDN',  'SDC'})
%title('V_MPP/V_opencircuit relations of');
print("MPP_relations.png","-color","-dpng")


%First Observation: with diaphragma higher relation  V_MPP/V_opencircuit, batteries more stables
%at operationg point with diaphragma
%Next: SDN! with a bit piece of zinc
```

Appendix C.

Electronic Implementation

C.1. The bq25504 adapter

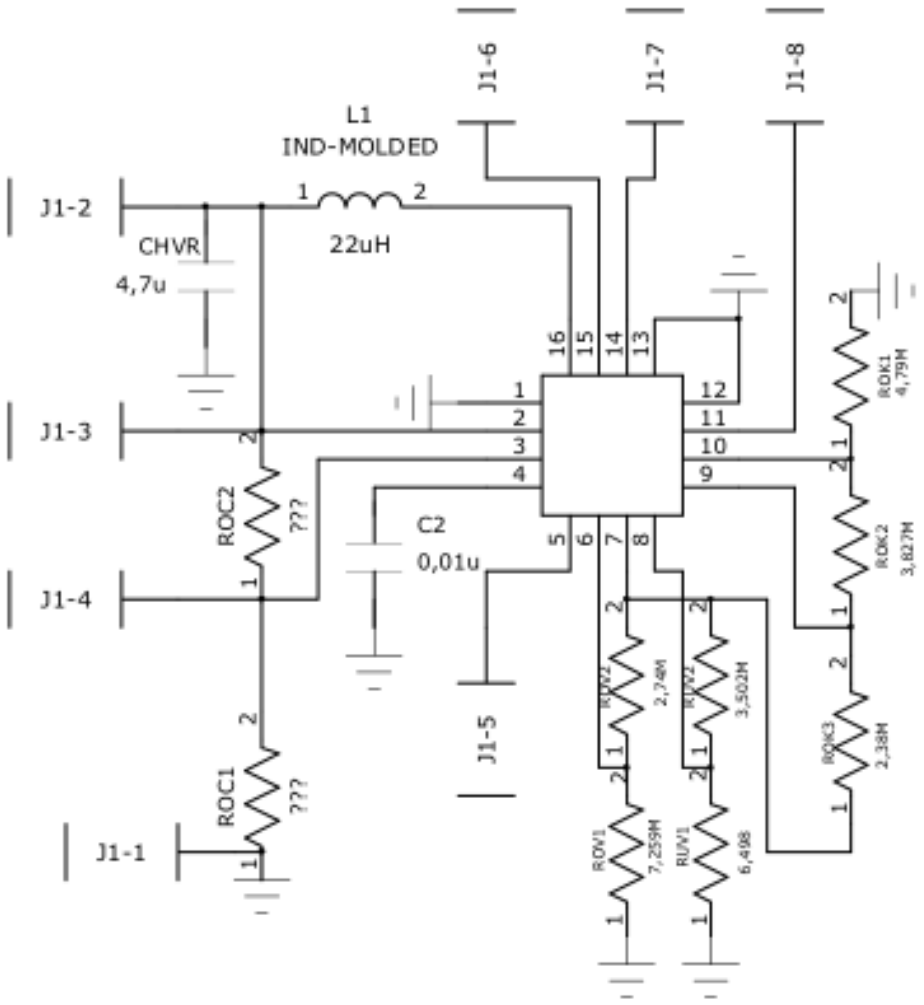

Figure C.1.: The schedule of the bq25504 adapter

This schedule is realized on a 2-layer PCB

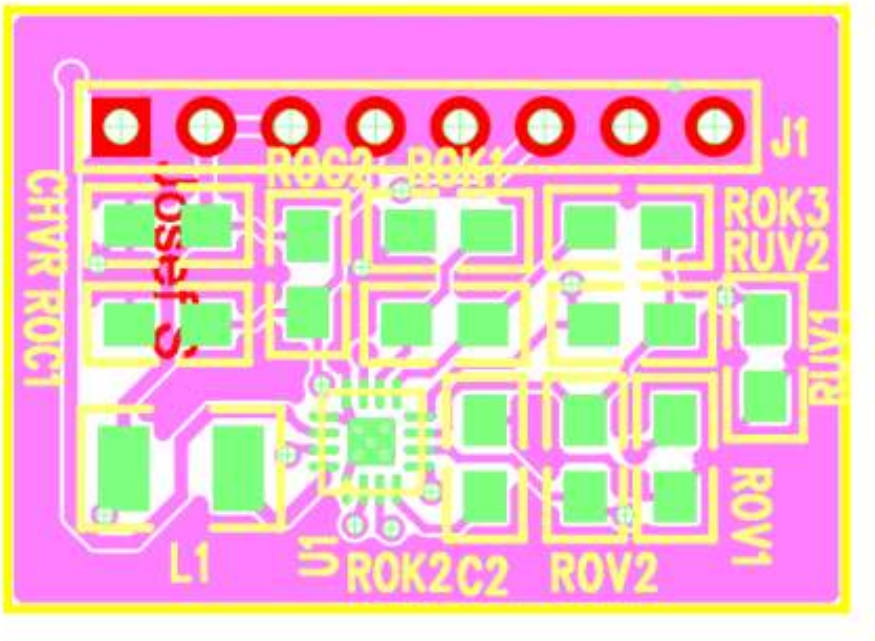

Figure C.2.: The top layer of the bq25504 adapter

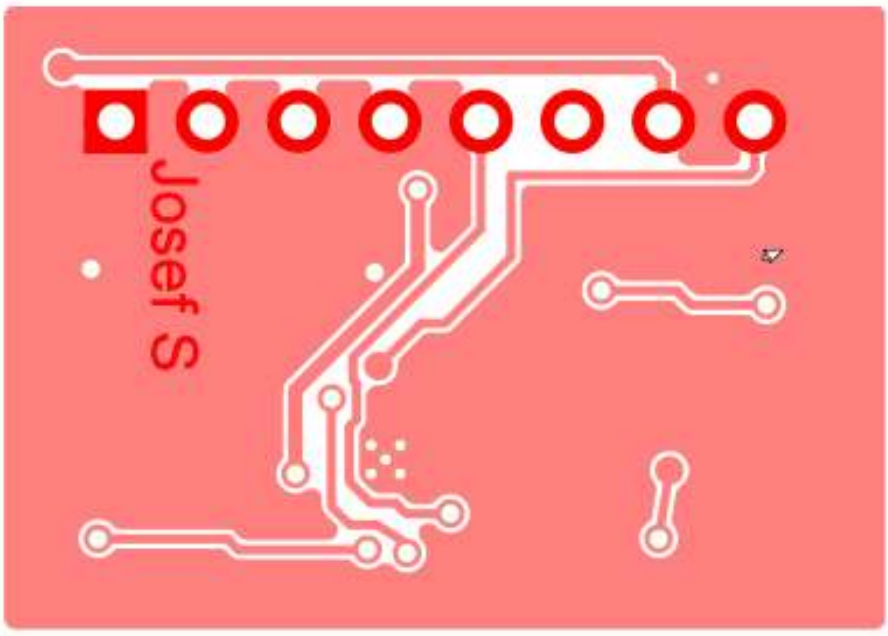

Figure C.3.: The bottom layer of the bq25504 adapter

C.2. Power Flower Bell ver. 0.1

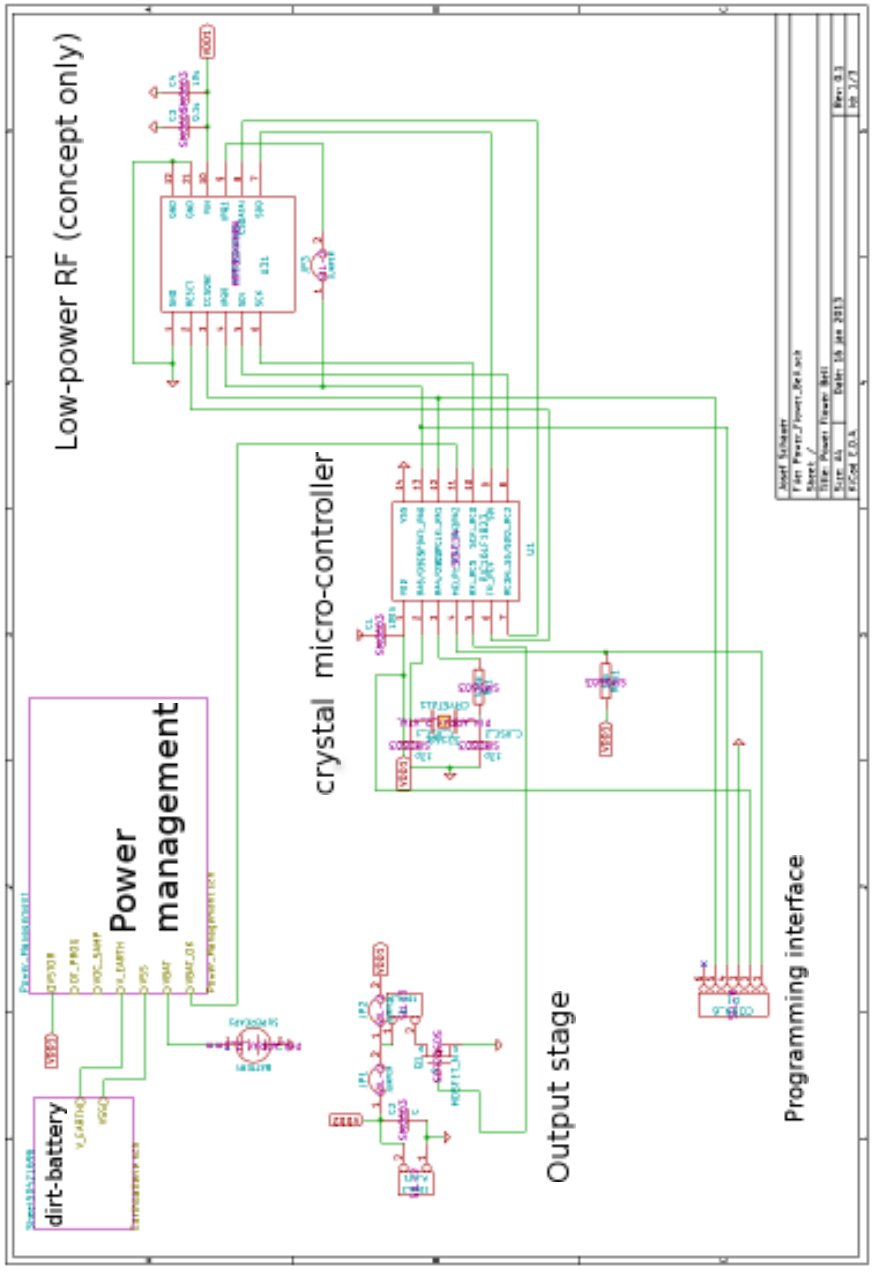

Figure C.4.: Schedule of the PFB

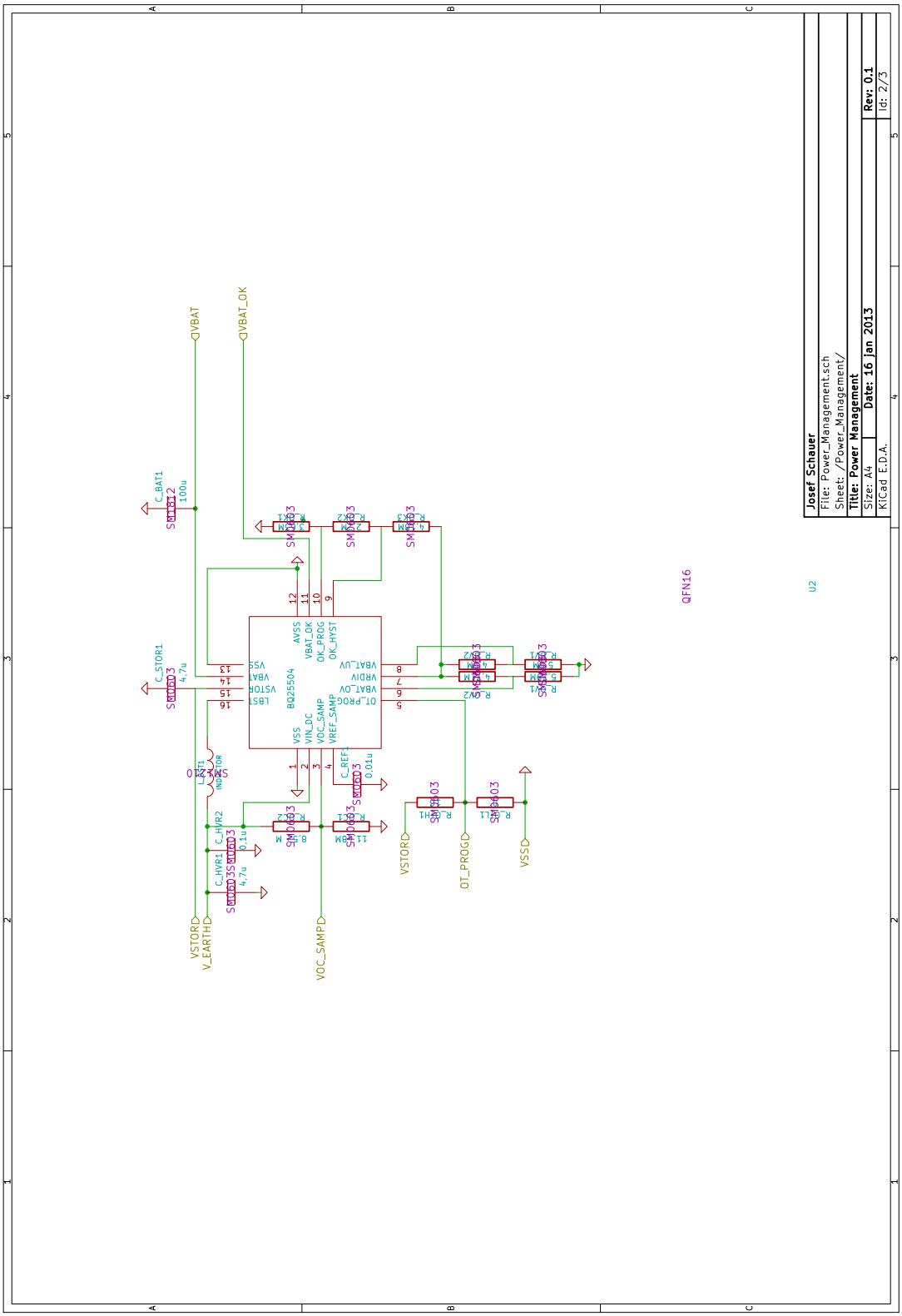

Figure C.5.: Schedule of the power management part of the PFB

Appendix D.

C-Source code for the PIC®16LF1823

D.1. PFB_Energy_Tester

```
/*
* File:   main.c
* Author: iem
*
* Created on 18. Juli 2012, 16:14
*/
#include <xc.h>
#include <stdio.h>
#include "config.h"
#include "hardwaredefs.h"
#include <pic16lf1823.h>
#include <delays.h>
#include "spi.h"
#include "system.h"
#include "usart.h"

//#include <stdlib.h>



// prototypes
void static init_hardware(void);
void static LED1_blink(void);
void putch(char data);
void VBAT_isr(void);                    // VBAT Interruptroutine

bit static LED1_blinken;


int main(void)
{
```

```
        init_hardware();
        LED1 = 0;

        while(1)
        {

            if(!VBAT_OK)
            {


            LED1 = 0;
            SLEEP();
            __delay_ms(20);

            }
            else LED1=1;


        }
    }
    /* Initialize Hardware */

    static void init_hardware(void)
        {
        FOSC_8MHz() ;
        //F_OSC_500kHz();
        //ConfigureOscillator(F_OSC_8MHz );
        OSCCONbits.SCS=0;
        OSCTUNEbits.TUN =0b100000;

        //I/Os konfigurieren
        //OUT_A2 = 0;// as Output

        //Out_Byte1 = 0;

        //SPI initialisieren
        SSP1STATbits.SMP = 0; //input data sampled at middle of data
            output time;
        SSP1STATbits.CKE = 1; //Transmit on active to idle state
        //SPI_EN = 0;
        SSP1CON1= 0b00110010; //S281 idle state of clock is a high
            level Datasheet SPI Master mode, clock = FOSC/64
        SSP1CON3 = 0b00010000;//BOEN = 1
        SPI_EN = 1;

        //I/Os konfigurieren
```

```
OUT_MRF89XA_RESET = 0; //as output to reset MRF89XA

TRISCbits.TRISC0 = 0;   //SCK in master is output -> cleared
TRISCbits.TRISC1 = 1;   //SDI is input -> set
TRISCbits.TRISC2 = 0;   //SDO in master is output -> cleared
TRISCbits.TRISC3 = 0;   // SS/ Data in master is output ->
    cleared
TRISAbits.TRISA4 = 0;   //CS_CONF in master is output ->
    cleared
TRISAbits.TRISA2 = 1;   //VBAT_OK

//Analoge Ins
ANSELA= 0b00000000;
ANSELC= 0b00000000;


//Alternative Pin function register
APFCONbits.SDOSEL = 0; //sdo IS ON RC2
APFCONbits.SSSEL = 1; //!SS is on RA0
APFCONbits.T1GSEL = 0; //T1G function is on RA4

//SPI konfigurieren
SSP1STATbits.SMP = 0; //input data sampled at middle of data
     output time;
SSP1STATbits.CKE = 1; //Transmit on active to idle state 0,0
     mode!
//SPI_EN = 0;
SSP1CON1= 0b00100010; //S281 idle state of clock is a low
    level Datasheet SPI Master mode, clock = FOSC/64
SSP1CON3 = 0b0001000;//BOEN = 1

//OPTION_REGbits.WPUEN   = 0; //individual control for every
     input
OPTION_REGbits.nWPUEN = 0; //Weak Pull-Ups are individual
WPUAbits.WPUA5 = 0; //weak pull-up on RA5 disabled
WPUAbits.WPUA2= 0; //weak pull-up on RA2 disabled
WPUAbits.WPUA3 = 0; //weak pull-up on RA3 enabled




CS_DATA = 0;
CS_CON = 0; //Configuration
//Interrupts
```

```
    INTCONbits.GIE = 0;         //Global Interrupts enabled
    INTCONbits.INTE = 1;        //INT-Pin Interrupt enabled
    INTCONbits.PEIE = 0;
    INTCONbits.IOCIE = 1;
  /*
    //Real Time Clock
    T1CONbits.nT1SYNC = 1;    //not syncronized to system clock
    T1CONbits.TMR1CS = 0b10; //CLKSRC for TMR1 is pin; 1OSCEN =
       1 has to be set for crystal!
    T1CONbits.T1CKPS = 0b00; //Prescaler = 1:1
    T1CONbits.T1OSCEN = 0b1; //enabling Oscillator for Timer 1,
       wait for enabling Timer 1
    __delay_ms(20);
    T1CONbits.TMR1ON = 0b1;   //Switching on Timer 1
    __delay_ms(20);
    T1GCONbits.TMR1GE = 0;    //
        //Disables all active peripheral interrupts
    PIE1bits.TMR1IE  = 0;     //Timer1 Interrupt Enabled
    PIR1bits.TMR1GIF = 0;     //Init of Interrupt

*/


}

static void LED1_blink(void)
          {
                mLED_On();
                __delay_ms(20);
                __delay_ms(20);
                __delay_ms(20);
                mLED_Off();
                __delay_ms(20);
                __delay_ms(20);
                __delay_ms(20);
            }


void putch(char data) {
while( ! TXIF)
continue;
TXREG = data;
}
```